differentiation of the human B cells in these mice in detail. Most of the human B cells in the peripheral blood of the hu-HSC NOG mice were IgM and/or IgD positive (Fig. 2A). Few $CD27^+$ B cells were detected, indicating that almost all the B cells were in a naive state (Fig. 2B). This phenotype was different from that of the human B cells in PBMCs obtained from normal healthy donors or cord blood, which clearly consisted of three major subsets: $IgM^+IgD^+CD27^-$-naive B cells, $IgM^+IgD^+CD27^+$-activated or non-switched memory B cells and IgD^-CD27^+ memory B cells (Fig. 2B).

The analysis of the human B cells in the spleen from the hu-HSC NOG mice for two developmentally regulated markers, CD24 and CD38, revealed an unusual accumulation of $CD24^{int/hi}CD38^{hi}$ immature B cells in the spleen (Fig. 2C). This $CD24^{int/hi}CD38^{hi}$ population comprised up to 60% (62.0 ± 13.8%, $n = 6$) of the splenic $CD19^+$ cells on average in the hu-HSC NOG mice. The frequency was lower at early time points after reconstitution but gradually increased; i.e. ~50% (53.3 ± 8.0%, $n = 3$) 6–8 weeks after reconstitution and ~70% (70.7 ± 13.7%, $n = 3$) 16 weeks after (Fig. 2D). Although a similar $CD24^{int/hi}CD38^{hi}$ population was also evident in the cord blood B cells or PBMCs (~30% or 2–3% in $CD19^+$ cells, respectively) (Fig. 2C), the $CD24^{int/hi}CD38^{hi}$ population in the hu-HSC NOG mice showed an even more immature phenotype (Fig. 2C); i.e. the former was $CD21^{hi}$ $CD23^{int}CD10^{lo}$ IgD^{hi}, while the latter was $CD21^-CD23^-CD10^{int/hi}IgD^{-/lo}$. Besides the $CD24^{int/hi}CD38^{hi}$ population, even when gated on more mature IgM^+ B cells, ~25% of the cells in the hu-HSC NOG mice were still $CD24^{hi}CD21^-IgD^{-/lo}$ (Fig. 2E), resembling the phenotype of transitional type 1 (T1) B cells (33). These analyses collectively suggested that the human B cells were only partially differentiated in the hu-HSC NOG mice.

Accumulation of B-cell precursors in the spleen of hu-HSC NOG mice

We also noticed the presence of a large number of $CD19^+CD24^{int/hi}CD38^{hi}IgM^-IgD^-$ cells (~40% of the $CD19^+$ population) in the spleen of the hu-HSC NOG mice (Fig. 3A, left panel). Because of their immature phenotype, we suspected these cells to be B-cell progenitors. Further dissection of the $CD19^+IgM^-IgD^-$ population using anti-CD20 and CD34 antibodies demonstrated that they consisted of at least three fractions: $CD20^-CD34^+$, $CD20^-CD34^-$ and $CD20^+CD34^-$ B cells (Fig. 3A, right panel). Since B cells with these phenotypes are known to comprise immature B-cell lineages in the BM, we examined the BM cells in the hu-HSC NOG mice. As expected, $CD19^+IgM^-CD20^-CD34^+$ pro-B and $CD19^+IgM^-CD20^-CD34^-$ pre-B cells were detected (Fig. 3B). The expression of CD179 (V_{preB}) and cytoplasmic μ chain (cμ) was also examined by intracellular staining. There were three distinct populations with different expression patterns for CD179 and cμ: $CD179^+c\mu^-$ pro-B, $CD179^+c\mu^+$ pre-B and $CD179^-c\mu^+$ populations, both in the spleen and BM (Fig. 3C and D). We obtained similar results for $V_{\lambda 5}$ (data not shown). RT-PCR analyses showed that the pro-B- or pre-B-like cells in the spleen expressed RAG and TdT, with patterns similar to those of the pro-B and pre-B cells in the BM (Fig. 3E).

In addition to the presence of phenotypically pro-B- and pre-B-like cells in the spleen of the hu-HSC NOG mice, further immature B-cell lineages, i.e. early-B cells or common lymphoid progenitors, were detected in the spleen. Using CD38 and CD10 (34, 35), a clear $CD19^-CD38^+CD10^+CD34^+$ early-B-cell population was detected in the spleen as well as in the BM (Fig. 3F and G). These results collectively suggest that early precursors in the B-cell lineage were present in the spleen of the humanized NOG mice.

IgG response of the human B cells from hu-HSC NOG mice to in vitro stimulation

The poor production of IgG in the hu-HSC NOG mice might have been attributed to the inappropriate differentiation of human B cells in the mouse environment. To examine the intrinsic capability of the B cells for the IgG response, we used an *in vitro* culture system. IgD^+CD19^+-naive mature B cells were purified from the spleen of hu-HSC NOG mice and stimulated with SAC as quasi-antigens in the presence or absence of anti-CD40 antibody. IL-21/IL-2 was also provided because these cytokines, especially IL-21, are potent inducers of naive B-cell differentiation into antibody-secreting cells *in vitro* (36, 37). Significant amounts of both IgM and IgG were detected in the supernatants after a 7-day culture (Fig. 4A). The IgG level was comparable to that of normal B cells from healthy donors (data not shown). Antigenic stimulation together with IL2/IL-21 also induced the formation of IgD^-CD38^+ antibody-secreting cells (Fig. 4B). In addition, IgD^-CD27^+ cells appeared toward the end of the culture period (Fig. 4B). The antibody class switch in these B cells was further supported by the induction of AID mRNA in the cultured B cells (Fig. 4C). These results suggested that the human B cells with a mature phenotype in hu-HSC NOG mice could respond to antigenic stimulation and had the functional molecular machinery for the Ig class switch.

Analysis of the human T cells in hu-HSC NOG mice: impaired function of $CD4^+$ T cells

Since the human B cells from hu-HSC NOG mice could produce IgG *in vitro*, we next examined the T cells in the hu-HSC NOG mice. The development of human $CD4^+$ and $CD8^+$ T cells was detected in the thymus and spleen of the hu-HSC NOG mice (Fig. 5A). Initially, we compared the expression patterns of several T-cell-related antigens and cytokine receptors: CD28, CD44, CD62L, CD132 (γc) and IL-7Rα chain (Fig. 5B). There were, however, no significant differences in these molecules between the T cells from the hu-HSC NOG mice and PBMCs.

To address the functionality of the T cells, we stimulated the whole-spleen cells from hu-HSC NOG mice with PHA or a mixture of soluble anti-CD3 and anti-CD28 antibodies in *in vitro* culture systems. The hu-HSC NOG spleen cells showed significant proliferation after 3 days in culture, consistent with previous reports (Fig. 5C). However, when the whole-spleen cells from the hu-HSC NOG mice previously immunized with KLH were re-stimulated in the presence of KLH *in vitro*, we could hardly detect IFN-γ and IL-4 (data not shown). This result was in agreement with the poor IgG production in the hu-HSC NOG mice.

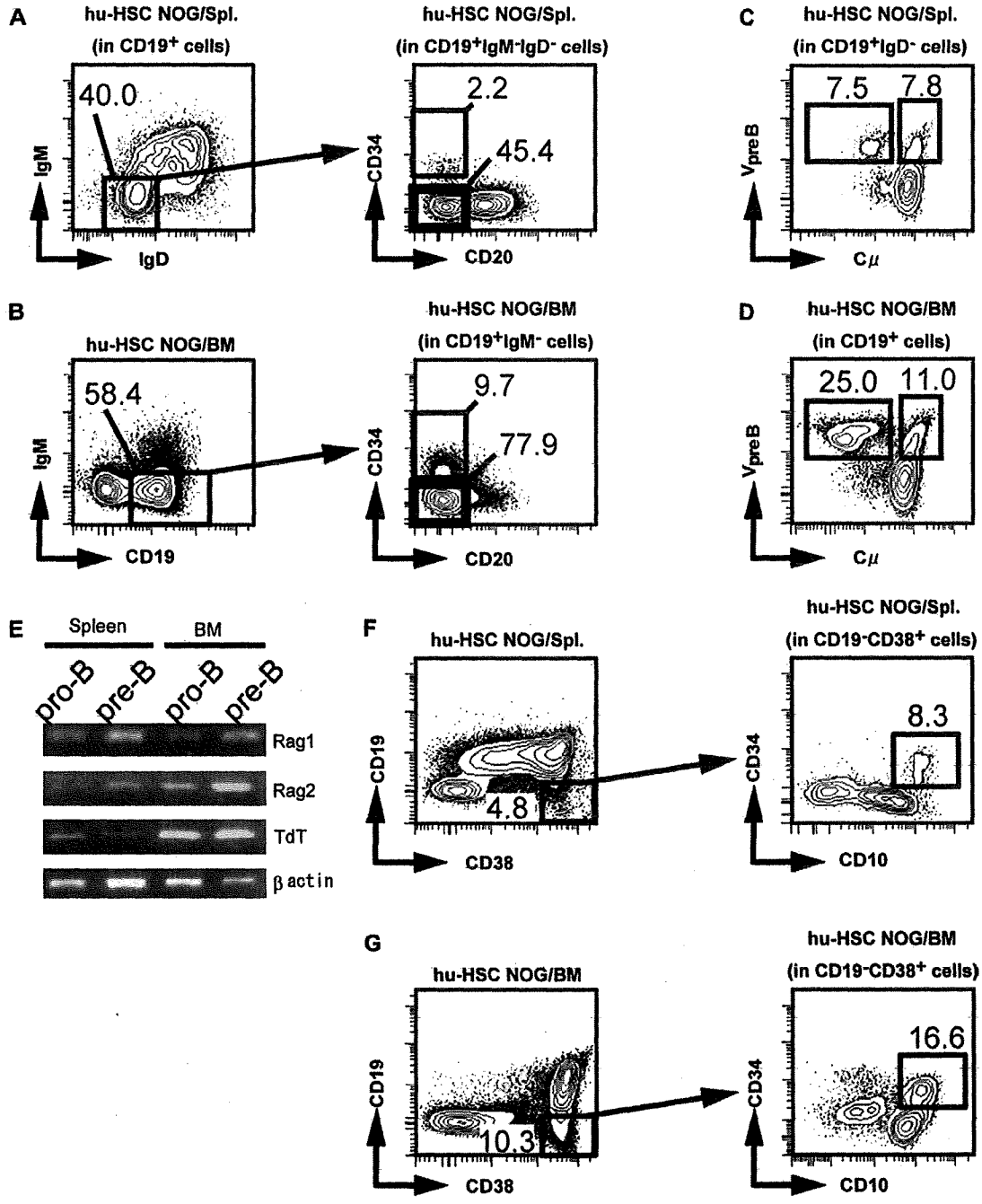

Fig. 3. Accumulation of human B-cell progenitors in the spleen of hu-HSC NOG mice. (A and B) Representative staining data of spleen (A) or BM (B) of hu-HSC NOG mice. The spleen cells or BM from hu-HSC NOG mice (8 weeks after reconstitution, $n = 4$) were stained with anti-CD19, anti-IgM and anti-IgD antibodies as described in Methods (left panels). The $CD19^+IgD^-IgM^-$ or $CD19^+IgM^-$ cells (represented by rectangles) in the spleen or BM, respectively, were further analyzed for the expression of CD34 and CD20. $CD34^+CD20^-$ (gated by thin rectangle) or $CD34^-CD20^-$ B cells (gated by bold rectangle) represent pro-B or pre-B cells, respectively. (C and D) Expression of V_{preB} in B cells in hu-HSC NOG mice. $CD19^+IgD^-$ cells in the spleen (C) or $CD19^+$ cells in BM (D) were examined for V_{preB} with cμ by intracellular staining (8 weeks after reconstitution, $n = 3$). The gated $V_{preB}{}^+c\mu^-$ or $V_{preB}{}^+c\mu^+$ cells represent pro-B cells or pre-B cells, respectively. (E) Analyses of gene expression in human B-cell progenitors in hu-HSC NOG mice. cDNA was prepared from $CD19^+IgM^-CD34^-CD10^+$ pre-B or $CD19^+IgM^-CD34^+CD10^+$ pro-B cells in the spleen or BM of the hu-HSC NOG mice (8 weeks after reconstitution). The expression of RAG-1, RAG-2 or TdT was examined by semi-quantitative RT-PCR as described in Methods. A representative result of three independent experiments is shown. (F and G) Detection of early-B cells in the spleen (F) or BM (G) in hu-HSC NOG mice. Cells were stained with anti-CD19 and anti-CD38 antibodies (left panels). The expression of CD10 and CD34 in $CD19^-CD38^+$ gated cells were further examined (8 weeks after reconstitution, $n = 3$). The gated $CD19^-CD38^+CD10^+CD34^+$ cells represent early-B or common lymphoid progenitors cells.

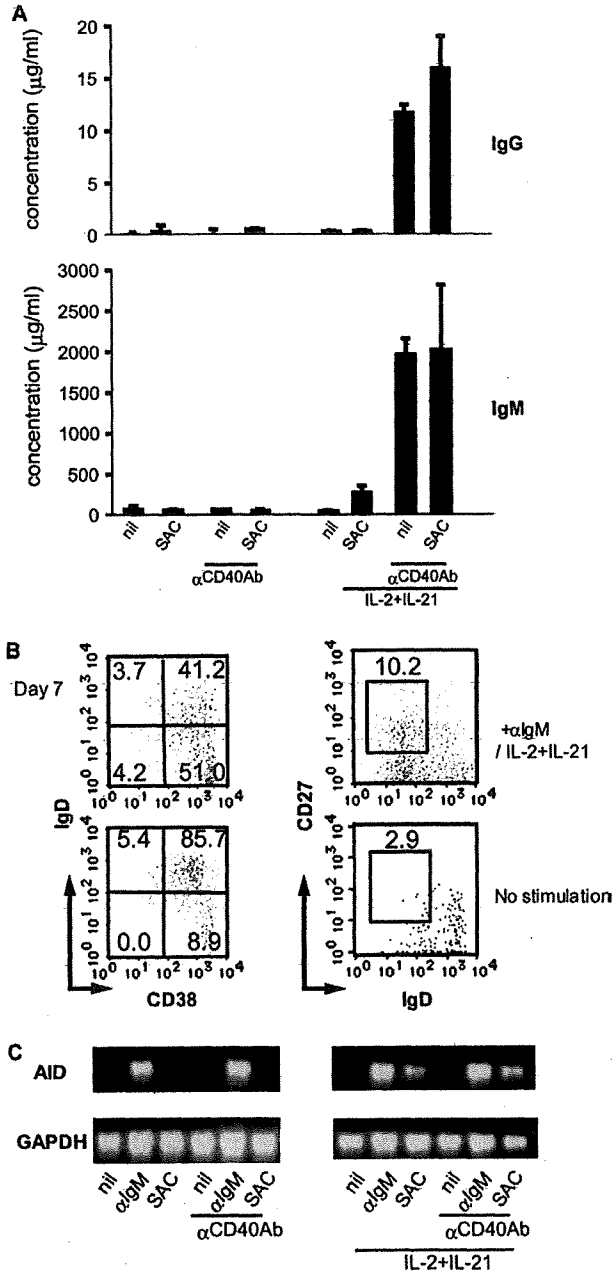

Fig. 4. Analysis of immune response of human B cells in hu-HSC NOG mice *in vitro*. (A) Purified IgD$^+$ splenic B cells in the hu-HSC NOG mice (8–16 weeks after reconstitution, $n = 4$) were stimulated *in vitro* with SAC (0.01%), in the presence or absence of anti-CD40 polyclonal antibody (1 μg ml^{-1}), with or without IL-2 (25 U ml^{-1})/IL-21 (100 ng ml^{-1}); secretion of IgM and IgG by 7-day cultured human B cells. Each culture supernatant was harvested and the amounts of human IgM (lower panal) and IgG (upper panel) were quantified by ELISA as described in Methods. (B) Analysis of surface antigen expression on CD19$^+$ splenic B cells in hu-HSC NOG mice (8–16 weeks after reconstitution) after *in vitro* stimulation with or without polyclonal anti-IgM antibody and cytokines. After 1-week culture, the B cells were recovered and stained with anti-CD38, anti-CD27 and anti-IgD antibodies. A representative result of three independent cultures is shown. (C) Total RNA was extracted from the B cells 3 days after *in vitro* culture with various stimulations, followed by synthesis of cDNA. The expression of AID or GAPDH was investigated by RT-PCR. A representative result of three independent cultures is shown.

Although we observed the activation of the spleen cells of the hu-HSC NOG mice, the magnitude was quite low compared with that of the cultured PBMCs. To exclude the contributions of antigen-presenting cells and analyze the T cells directly, we used purified CD4$^+$ and CD8$^+$ T cells. When the purified T cells were stimulated with immobilized anti-CD3 and anti-CD28 antibodies, they showed significant proliferation compared with the culture without stimulation. However, the intensity of their response, especially that of the CD4$^+$ T cells, was markedly lower than that of normal T cells isolated from PBMCs (Fig. 6A, left panel). The cumulative data showed that the magnitude of the proliferation of CD4$^+$ T cells from the hu-HSC NOG mice was no more than 10% of the normal CD4$^+$ T-cell response (Fig. 6A, right panel). For the CD8$^+$ T cells, the tendency was less clear because there was a large variance among mice (Fig. 6A). The T cells from the hu-HSC NOG mice also showed only modest proliferation even when they were strongly stimulated with PMA and ionomycin (Fig. 6B). The amount of IL-2 produced by the cultured T cells was remarkably low, consistent with their low proliferation (Fig. 6C). Addition of exogenous IL-2 (100 IU ml^{-1}) did not restore the proliferation of the human T cells from the hu-HSC NOG mice (data not shown).

Mechanisms of the impaired response of the human T cells in hu-HSC NOG mice

To examine the mechanisms of the hyporesponse of the T cells in the hu-HSC NOG mice, we analyzed the expression of CD25 and CD69 after stimulation. These molecules were detected on both CD4$^+$ and CD8$^+$ T cells, at similar levels as on normal T cells from PBMCs (Fig. 7A). When the number of viable cells was enumerated, however, there were significant differences between the hu-HSC NOG T cells and PBMC T cells. AnnexinV and propidium iodide (PI) staining of cultured T cells demonstrated that >50% of the CD4$^+$ T cells from hu-HSC NOG mice were dead at 24 h, while only 10% of the PBMC T cells were (Fig. 7B). At 48 h, nearly 80% of the CD4$^+$ T cells from hu-HSC NOG mice were PI positive. The CD8$^+$ T cells showed different patterns among mice. In the half of the animals, nearly 80% of the CD8$^+$ T cells died after a 24-h culture, while in the remaining half, 60% of the cells were still alive after a 72-h culture (Fig. 7C). To investigate the higher susceptibility of the T cells in the hu-HSC NOG mice to cell death, we examined the expression of CD95 (Fas) and CD178 (FasL) on the T cells. A significant expression of CD95 (Fig. 7D) but not CD178 (data not shown) was detected on the T cells from the hu-HSC NOG mice. In the human T cells from PBMCs, there were two populations, CD95$^+$ and CD95$^-$, while in the hu-HSC NOG mice, most of the T cells expressed similar amounts of CD95 on their surface (Fig. 7D).

We next addressed whether the impairment of T-cell functions was already conferred to the T cells in the thymus of the hu-HSC NOG mice. CD4$^+$CD8$^-$ single-positive (SP) thymocytes were prepared from the hu-HSC NOG mice. Because the number of thymocytes in a hu-HSC NOG mouse was usually not sufficient for analysis, we introduced the *bcl-2* gene into the CD34$^+$ stem cells by retrovirus *in vitro* before transplantation in an effort to increase the cell number. Indeed, in such hu-HSC (*bcl-2*) NOG mice, the

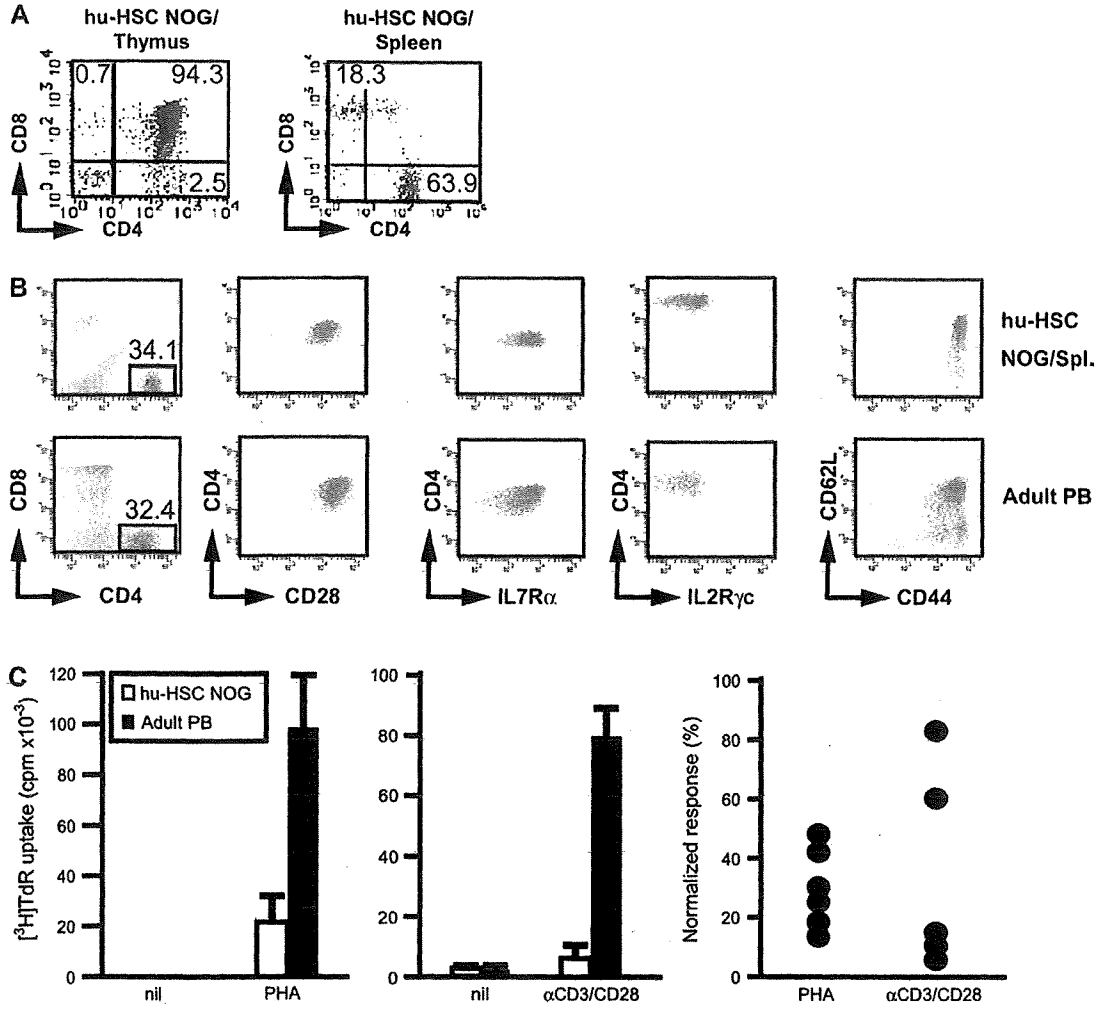

Fig. 5. Analysis of human T cells developed in hu-HSC NOG mice. (A) Development of human T cells in the thymus and spleen in hu-HSC NOG mice. Single-cell suspensions from each organ were stained with anti-CD4 and anti-CD8 antibodies (20 weeks after reconstitution, $n = 4$). (B) A representative staining for various molecules on human T cells from hu-HSC NOG mice. Whole-spleen cells from the hu-HSC NOG mice (20 weeks after reconstitution, $n = 3$) or adult peripheral blood (PB) were stained with indicated antibodies. $CD4^+$ T-cell population (gated by rectangles and highlighted by red dot plots) was further examined for each molecule. (C) Analysis of functions of human T cells in hu-HSC NOG mice *in vitro*. Whole splenocytes from the hu-HSC NOG mice (20 weeks after reconstitution) (white bar) or normal adult PB (black bar) were stimulated with PHA (left panel, $n = 6$) or mixture of soluble anti-CD3 and anti-CD28 antibodies (middle panel, $n = 5$). After 72-h culture, the proliferation of T cells was measured as the amounts of incorporated [^{3}H]thymidine ([^{3}H]TdR). Representative data are shown. The means from triplicated cultures are shown. The cumulative data are shown after normalizing the magnitude of the response of hu-HSC NOG T cells to that of PB T cells (right panel).

exogenous Bcl-2 was expressed at a high level (Fig. 8A), and the effect on increasing the thymocytes was remarkable (no more than 1×10^6 in each mouse with control GFP vector versus ~6×10^6 in *bcl-2* group), although the differentiation of B or T cells in the spleen was not affected (data not shown). We isolated the $CD4^+CD8^-$ SP thymocytes or splenic $CD4^+$ T cells from the hu-HSC (*bcl-2*) NOG mice and stimulated them as described above. The $CD4^+CD8^-$ SP cells showed vigorous proliferation, as high as that of normal T cells from PBMCs (Fig. 8B). A significant amount of IL-2 was also detected in the culture supernatants of the $CD4^+CD8^-$ SP cells (Fig. 8C). Interestingly, the splenic $CD4^+$ T cells from the same mice did not show proliferation (Fig. 8B). Consistently, immunization of the hu-HSC (*bcl-2*) NOG mice did not evoke an immune response in spite of the improvement in cell number (data not shown). Thus, the unresponsiveness of the T cells in the hu-HSC NOG mice was induced in the periphery, not in the thymus. Notably, the $CD4^+$ T cells from the hu-HSC (*bcl-2*) NOG mice showed better viability compared with the $CD4^+$ T cells from the usual hu-HSC NOG mice; 60–80% of the cultured cells were still viable after 48 h (data not shown). Hence, the poor response of the T cells from hu-HSC NOG mice was not solely due to their high susceptibility to cell death, but other mechanisms (such as induction of anergy) were also involved.

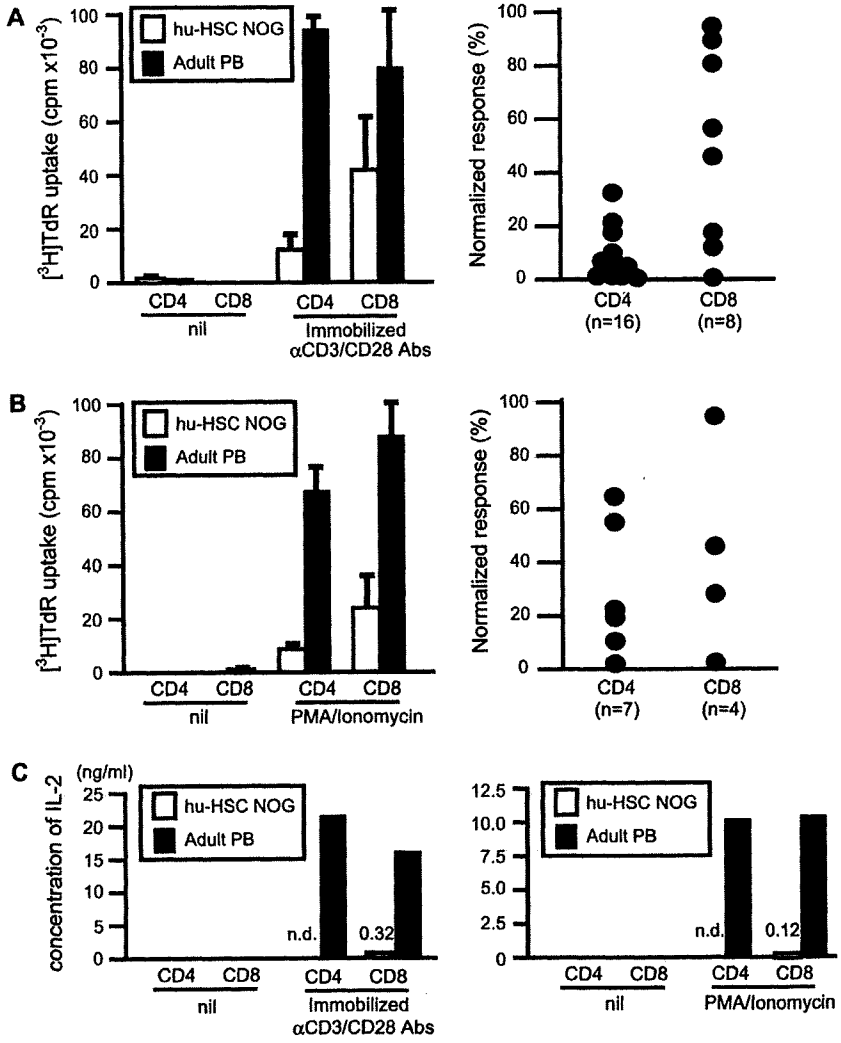

Fig. 6. Impaired responses of human T cells in hu-HSC NOG mice to mitogens. (A and B) Analysis of functions of human $CD4^+$ or $CD8^+$ T cells in hu-HSC NOG mice *in vitro*. $CD4^+$ or $CD8^+$ T cells were prepared from the spleen of the hu-HSC NOG mice (20 weeks after reconstitution) (white bar) or normal adult peripheral blood (PB) (black bar) as described in Methods. They were stimulated with immobilized anti-CD3 and anti-CD28 antibodies (A, left panel, $n = 16$ or 8 for $CD4^+$ T cells or $CD8^+$ T cells, respectively) or combination of PMA and ionomycin (B, left panel, $n = 7$ or 4 for $CD4^+$ T cells or $CD8^+$ T cells, respectively). After 72-h culture, the proliferation of T cells was measured as the amounts of incorporated [^{3}H]thymidine ([^{3}H]TdR) as in Fig. 5(C). The cumulative data are shown after normalizing the magnitude of the response of hu-HSC NOG T cells to that of PB T cells (right panels). (C) Quantification of IL-2 produced by human T cells in hu-HSC NOG mice *in vitro*. The amount of IL-2 in the supernatants obtained from the *in vitro* cultures described in (A and B) was measured by ELISA. n.d.: under detection level by ELISA.

Development of human T cells in NOG I-Aβ$^{-/-}$ mice

The results with the $CD4^+CD8^-$ SP thymocytes suggested that there were regulatory mechanisms to induce tolerance to the human T cells in the mouse periphery. To examine the involvement of mouse MHC molecules, we used the NOG I-Aβ$^{-/-}$ strain. In these mice, we could not detect any mouse $CD4^+$ T cells, as previously reported. Upon humanization, surprisingly, human T cells could be detected in the spleen of the hu-HSC NOG I-Aβ$^{-/-}$ mice (Fig. 9A). Thus, the HLA class II molecules on the human T cells (38) or a quite small number of human B cells or human dendritic cells (DCs) in the thymus positively selected human T cells in the mouse thymus. Although we could not detect a significant number of $CD4^+CD8^-$ SP thymocytes in the hu-HSC NOG I-Aβ$^{-/-}$ mice by FACS analysis after 20 weeks of reconstitution (Fig. 9B), these $CD4^+$ T cells were not derived from extrathymic tissues because no human T cells appeared in hu-HSC NOG *nu/nu* mice (data not shown), suggesting that the mouse thymus was indispensable for the human T-cell development. The number of $CD4^+$ T cells in the spleen was <1% of that in the regular hu-HSC NOG mice at 16 weeks after reconstitution and reached 20% at ~20 weeks (4.9×10^5, $n = 15$, in the regular hu-HSC NOG versus 1.2×10^5, $n = 4$, in the hu-HSC NOG I-Aβ$^{-/-}$ NOG). It is uncertain whether this increase was caused by the homeostatic proliferation

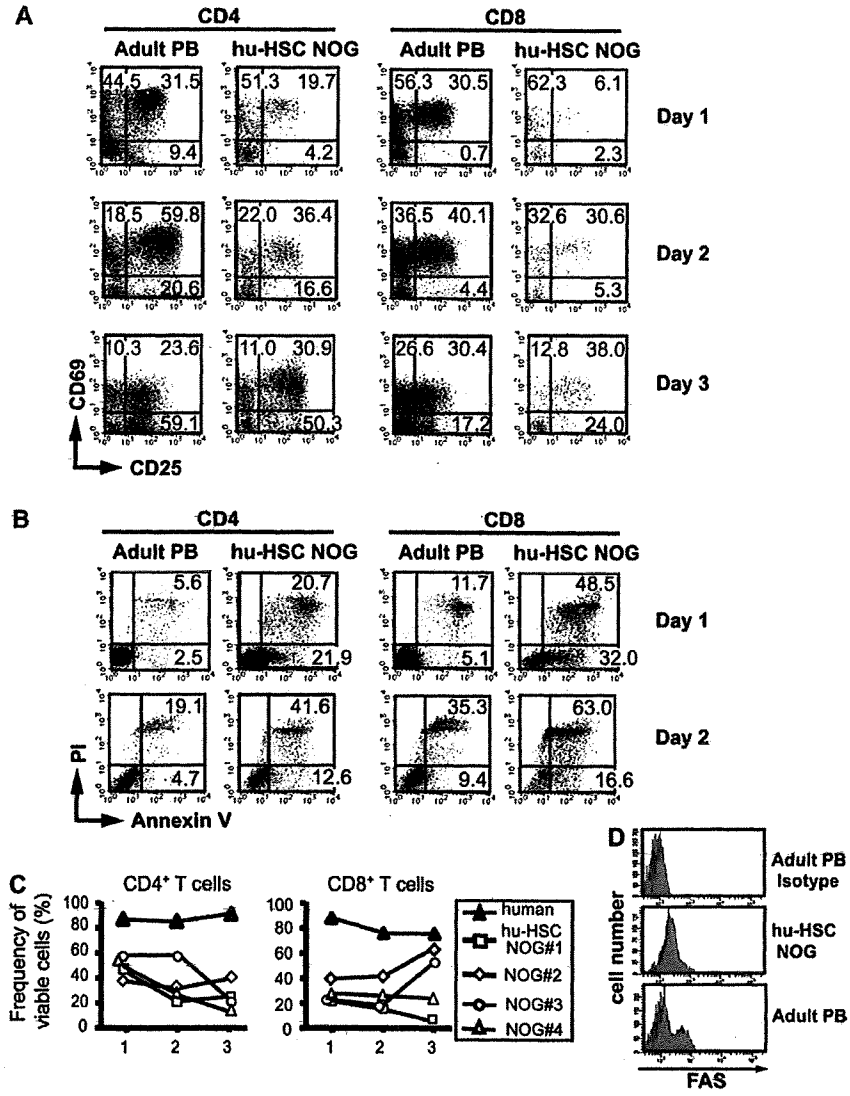

Fig. 7. Enhanced cell death of hu-HSC NOG T cells. (A) Analysis of activation markers of T cells. Purified $CD4^+$ or $CD8^+$ T cells from hu-HSC NOG mice (20 weeks after reconstitution) or human peripheral blood (PB) were stimulated by immobilized anti-CD3 and anti-CD28 antibodies as described in Fig. 6. The expression of CD25 and CD69 on them were analyzed every 24 h. A representative result from three independent animals is shown. (B) Analysis of apoptosis induced in T cells. The *in vitro* cultured $CD4^+$ or $CD8^+$ T cells as in (A) were stained with annexin V and PI at 24 and 48 h. A representative result from four independent experiments is shown. (C) Survival curve of *in vitro* cultured T cells. The frequency of viable $CD4^+$ or $CD8^+$ T cells was represented as the percentage of annexin V and PI double-negative cells in the FACS analysis mentioned in (B). (D) Expression analysis of CD95 (Fas) on T cells. A representative result of staining with anti-CD95 antibody is shown.

of peripheral T cells or the accumulation of migrated T cells from the thymus. Due to the low number of $CD4^+$ T cells in the hu-HSC NOG I-A$\beta^{-/-}$ mice that could be purified for *in vitro* experiments, we instead stimulated the whole-spleen cells from these mice with anti-CD3 and anti-CD28 antibodies *in vitro* after CFSE labeling to examine their responsiveness. The dilution of CFSE in the T-cell population was measured on days 4 and 6. The human T cells in the hu-HSC NOG I-A$\beta^{-/-}$ mice showed no significant proliferation (Fig. 9C). Thus, the human T cells that developed in the absence of I-A were also rendered unresponsive.

IgG response in hu-HSC NOG mice upon the adoptive transfer of normal T cells

Our analyses revealed that the hu-HSC NOG mice have problems in both their B-cell and T-cell populations. However, since the B cells could mount an IgG response, if not complete, to *in vitro* stimulation, we next examined whether antigen-specific IgG responses were possible *in vivo*, if supplemented with functional T cells. For this purpose, we used a TCR specific for an HA peptide ($HA_{307-319}$) that was derived from an HA-specific human T-cell clone, B16 (31). The TCR was introduced into human T cells isolated from PBMCs by retroviral vectors (Fig. 10A). The expression of the

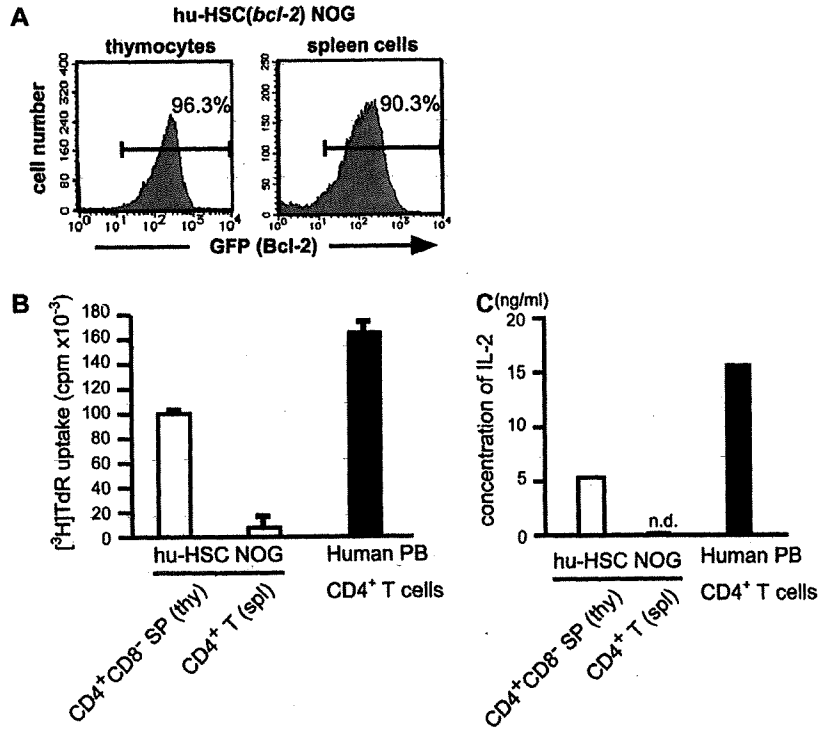

Fig. 8. Normal response of $CD4^+CD8^-$ SP thymocytes from hu-HSC NOG mice. (A) Reconstitution of hu-HSC (*bcl-2*) NOG mice. A representative analysis for expression of exogenous *bcl-2* represented by bicistronic GFP from retroviral vector in thymocytes and spleen cells. The thymocytes and spleen cells were prepared from the hu-HSC (*bcl-2*) NOG mice 20 weeks after reconstitution and examined the expression of GFP ($n = 6$). (B) Analysis of functions of human $CD4^+CD8^-$ SP thymocytes in hu-HSC (*bcl-2*) NOG mice *in vitro*. $CD4^+CD8^-$ SP thymocytes were prepared from pooled thymuses from five different hu-HSC (*bcl-2*) NOG mice grafted with the same $CD34^+$ cells (20 weeks after reconstitution). $CD4^+$ T cells were also purified from the same hu-HSC (*bcl-2*) NOG mice. These NOG-derived T cells (white bar) or normal adult peripheral blood (PB) (black bar) were stimulated with immobilized anti-CD3 and anti-CD28 antibodies. After 72-h culture, the proliferation of T cells was measured as the amounts of incorporated [^{3}H]thymidine ([^{3}H]TdR) as mentioned in Fig. 5(C). Representative data from three independent experiments are shown. (C) Quantification of IL-2 produced by human $CD4^+CD8^-$ SP thymocytes in hu-HSC (*bcl-2*) NOG mice *in vitro*. The amount of IL-2 in the supernatants obtained from the *in vitro* cultures described in (B) was measured by ELISA. n.d.: under detection level by ELISA.

antigen-specific TCR was also confirmed by staining with the specific tetramer (HLA-DRB1*0401/$HA_{307-319}$) (Fig. 10B). The transduced T cells produced IL-2 in response to the antigenic stimulation by a B-cell lymphoma cell line (*HLA-DRB1*0401* positive) loaded with the $HA_{307-319}$ peptide (Supplementary Figure S1, available at *International Immunology* Online). Because the B16 TCR is restricted by HLA-DR4 (DRB1*0401) and the frequency of this haplotype in the Japanese population is quite low (~1% of the population), the *HLA-DRB1*0401* gene was introduced into $CD34^+$ stem cells by retrovirus to obtain hu-HSC [HLA-DR4 (DRB1*0401)] NOG mice (Fig. 10C). We then transferred the human T cells containing the B16 TCR into the hu-HSC [HLA-DR4 (DRB1*0401)] NOG mice and immunized them with the $HA_{307-319}$ peptide (Fig. 10D). After repeating the transfer and subsequent antigenic challenges twice, we measured the amount of IgG specific for the HA peptide. Although the total IgG level in the sera was markedly elevated after immunization, the titer of HA peptide-specific IgG remained low (Fig. 10E). The increase in total IgG occurred through non-specific activation of the B-cell population by the B16 TCR-bearing human T cells, suggesting that the machinery for Ig class switch is also functional *in vivo*. We could not, however, detect any donor human T cells with the B16 TCR by staining with the specific tetramer (data not shown) 10 days after the final antigenic challenge, which may explain the absence of the HA-specific IgG response in the hu-HSC [HLA-DR4 (DRB1*0401)] NOG mice.

Discussion

In this study, we have clarified the possibilities and limitations of the present humanized mouse technology. The quasi-human immune system in humanized mice has been shown to be relatively similar to *bona fide* human immunity (5–9). However, the induction of successful immune reactions against exogenous antigens, especially the humoral responses represented by IgG responses, has been a high hurdle for humanized mice (21, 22, 24, 25). Several mechanisms have been suggested for this defect, including the skewing of human B cells toward the B-1 cell lineage (24), and the lack of interactions between B and T cells due to mismatches of the MHC (24). Our results suggest that in addition to these possibilities, other previously unrecognized mechanisms involving both B and T cells are also responsible for this limitation.

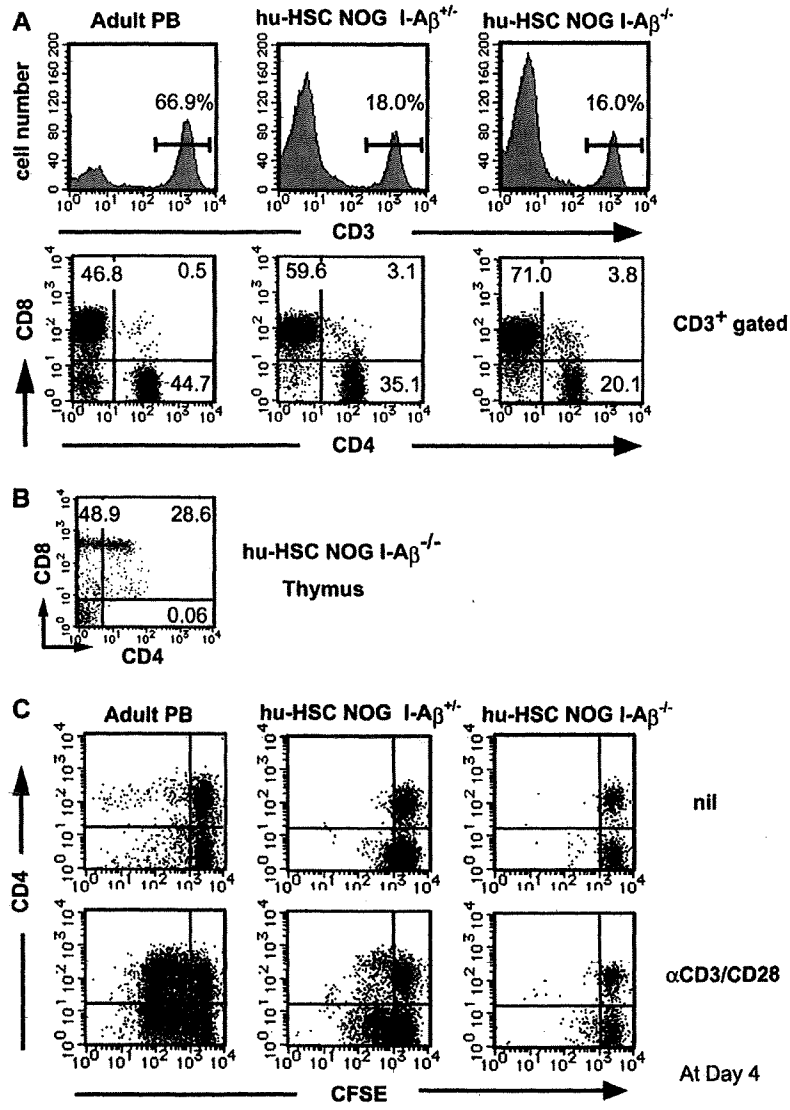

Fig. 9. Analysis of human T cells developed in hu-HSC NOG I-Aβ$^{-/-}$ mice. (A) NOG I-Aβ$^{+/-}$ or NOG I-Aβ$^{-/-}$ mice were reconstituted with human CD34^{+} stem cells as described in Methods. Adult peripheral blood (PB) or the whole-spleen cells from respective humanized mice (20 weeks after reconstitution) were stained with anti-CD3 antibody (top panel). The CD3-positive cells were further stained with anti-CD4 and CD8 antibodies (bottom panels). A representative staining of four independent experiments is shown. (B) Development of thymocytes in hu-HSC NOG I-Aβ$^{-/-}$ mice. The pooled thymocytes from three NOG I-Aβ$^{-/-}$ mice (20 weeks after reconstitution) were stained with anti-CD4 and CD8 antibodies. (C) Analysis of functions of human CD4^{+} T cells in the hu-HSC NOG I-Aβ$^{-/-}$ mice *in vitro*. The whole-spleen cells from the hu-HSC NOG I-Aβ$^{+/-}$ or hu-HSC NOG I-Aβ$^{-/-}$ mice (20 weeks after reconstitution) or adult PB were stained with CFSE, subsequently cultured in the presence of anti-CD3 and anti-CD28 antibodies. The cultured cells were recovered on day 4 and stained with anti-CD4 and anti-CD8 antibodies. The intensity of CFSE in CD4^{+} or CD8^{+} T cells was examined by FACS. A representative result from three independent experiments is shown.

The function of the 'mature' human IgD^{+} B cells in hu-HSC NOG mice is reasonable, considering that they had an IgG response *in vitro* and *in vivo*. In contrast, there were at least three major obstacles on the T-cell side. The first was the T cells' high susceptibility to cell death. The second was their unresponsiveness, represented by their low proliferation and low production of IL-2. The third was the poor maintenance of human T cells in the mouse environment. However, several other regulatory mechanisms would be present that could also induce the loss of human T-cell function in the mouse periphery. These functional abnormalities contradict previous reports suggesting that functional human T cells develop in humanized mice, although those studies did not analyze the functions in detail (20, 22, 39, 40).

Our results using hu-HSC (*bcl-2*) NOG mice, in which the thymocytes were reactive while the splenic T cells were not, suggested that although human T cells are positively selected in the mouse thymus, they lose their function mainly in the periphery. Given the normal positive selection of human T cells in the mouse thymus, why are they compromised

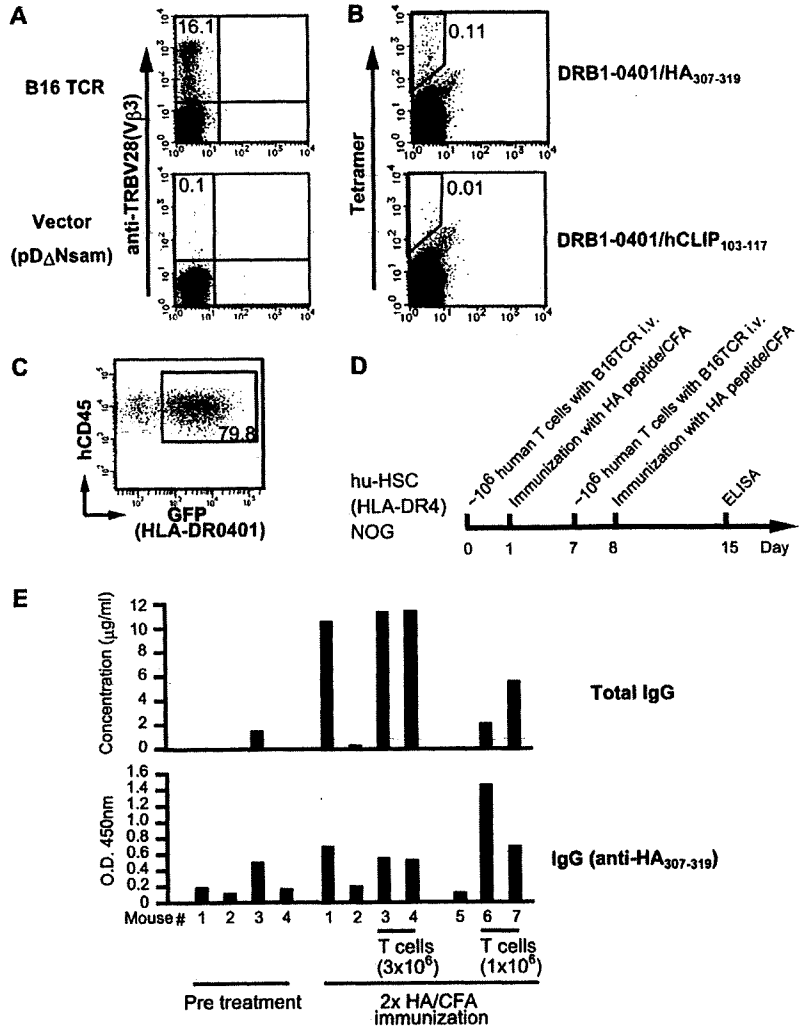

Fig. 10. Induction of IgG in hu-HSC NOG mice. (A) Retroviral delivery of $HA_{307-319}$ peptide-specific TCR (B16) into normal human T cells. Purified human T cells from normal healthy donor were activated *in vitro* as described in Methods. The T cells were subsequently spun infected with retrovirus encoding B16 TCR. The expression of B16 TCR was determined by anti-TRBV28 antibody after 10 days. (B) The frequency of the T cells with B16 TCR was further determined by staining with the specific (middle panels) or irrelevant (right panels) tetramers. (C) Reconstitution of hu-HSC [HLA-DR4 (DRB1*0401)] NOG mice. The expression of the exogenous *HLA-DRB*0401* gene in peripheral blood cells from hu-HSC [HLA-DR4 (DRB1*0401)] NOG mice was represented by bicistronic GFP from retroviral vector (8 weeks after reconstitution, $n = 6$). (D) The schema of experiments for inducing IgG in the hu-HSC [HLA-DR4 (DRB1*0401)] NOG mice upon transfer of B16 TCR-bearing human T cells. (E) Quantification of total IgG or peptide-specific IgG in the hu-HSC [HLA-DR4 (DRB1*0401)] NOG mice. One week after final antigenic challenge, the sera were collected form the mice. Total IgG (left panel) and HA-specific IgG (right panel) were measured by ELISA after 10-fold dilution of the specimens. The results from three or four different mice in each group were shown.

in the periphery? It has been controversial whether the mouse MHC on mouse thymic epithelial cells or the HLA molecules on human BM-derived cells are responsible for the thymic selection of human T cells in the hu-HSC NOG mouse. The significant delay of human T-cell development in hu-HSC NOG I-A$\beta^{-/-}$ mice suggests that the I-A on mouse epithelial cells plays a major role in the positive selection, admitting that a small number of human $CD4^+$ T cells could still develop in the absence of I-A. In this setting, there are two possibilities. The first is that human T cells are not subjected to proper negative selection by human molecules that are not present in the mouse thymus. Indeed, structural analyses of the thymus of hu-HSC NOG mice showed incomplete formation of the cortex where negative selection occurs (Supplementary Figure S2, available at *International Immunology* Online) (41). In this situation, human T cells would be inappropriately activated by I-A/human molecule-derived peptide complexes on the mouse antigen-presenting cells without the proper co-stimulations due to the barrier of species, rendering a refractory state. The second possibility is that human B cells induce unresponsiveness in the T cells because they are not professional antigen-presenting cells; that is, there is a xenoreaction to the HLA molecules on B cells by the human T cells selected by mouse MHCs.

The poor development and differentiation of human professional antigen-presenting cell like DCs and macrophages in hu-HSC NOG mice may also support this possibility (Supplementary Figure S3, available at *International Immunology* Online). The induction of the refractory state of the human T cells might be attributed to one or both of these mechanisms. As for the high susceptibility to cell death of the human T cells in hu-HSC NOG mice, a previous report suggested the high turnover of human T cells in humanized mice (42). The proliferation would be attributed, in part, to the lymphopenic situation in mouse environment where the number of human T cells is very low. Under the condition, it is possible that the human T cells in hu-HSC NOG mice become susceptible to FAS-mediated cell death (43).

The involvement of mouse I-A in the induction of the refractory state of human T cells in hu-HSC NOG mice might be tested using the hu-HSC NOG I-A$\beta^{-/-}$ mice because they developed human T cells. However, because these T cells had impaired function, the involvement of I-A remains to be determined. The results in hu-HSC NOG I-A$\beta^{-/-}$ mice might suggest that in the absence of class II on thymic epithelial cells, the positive selection of human T cells was simply incomplete or that other mechanisms were responsible for inducing abnormalities in the T cells besides the two described above. To circumvent these problems, it is necessary to construct environments in which there is no interference from mouse class II and from which a sufficient number of human T cells can still be obtained. One possibility might be to combine NOG I-A$\beta^{-/-}$ mice with BLT technology, in which an organoid consisting of pieces of fetal thymus and liver are implanted into mice with the subsequent transfer of $CD34^+$ stem cells from the same donor (44). As an alternative approach, the total replacement of mouse co-stimulatory molecules (CD80, CD86, ICAM-1, ICAM-3, etc.) and class II molecules with human orthologues might be useful.

The maintenance of human T-cell functions in the mouse environment is also important. Previous reports using hu-PBL NOD/scid mice showed that normal human T cells lose their capacity to be activated at a certain period after transplantation (45). In our study, the human T cells bearing an HA-specific TCR did not show any expansion, even after repeated immunization with the specific peptide. Supplementing the mouse model with human cytokines could be a strategy for keeping the human T cells viable and functional.

We found at least two abnormal aspects of the B-cell population in the hu-HSC NOG mice. One was a blockage of the differentiation of B cells around the transitional stage and the other was the unusual appearance of B-cell precursors in the spleen. Nevertheless, our functional analyses suggested that the differentiation and functions of the B cells were relatively close to normal. Further studies examining the B-cell function *in vivo* (e.g. expansion capacity, affinity maturation and differentiation into memory or plasma cells) must be undertaken, and additional efforts are necessary to achieve the full maturation of human B cells in mice. We believe that the hu-HSC NOG mice could be developed into a good model for studying the mechanisms involved in the proper differentiation of human B cells.

Humanized mice are becoming common tools for studying human immunity and its related diseases (46, 47). Knowledge has been accumulating about the molecular mechanisms that regulate the development and functions of hematopoietic cells in both humans and mice. It will be important to examine this information using improved model systems, for example, by creating various transgenic NOG strains that are supplemented with human cytokines or growth factors. More sophisticated humanized mice, if achieved, would lead to a better understanding of human immunity and the development of effective therapeutic treatments for human diseases involving autoimmunity or human-specific viral infections.

Supplementary data

Supplementary Figures S1–S3 are available at *International Immunology* Online.

Funding

Ministry of Education, Culture, Sports, Science and Technology of Japan and Japan Society for the Promotion of Science to K.S. (19059001) and M.I. (18100005); Takeda Scientific Foundation to T.T.

Acknowledgements

We thank K. Murata and M. Ito for the technical assistance and their secretary jobs. The authors have no financial conflict of interest.

Abbreviations

APC	allophycocyanin
BM	bone marrow
CFSE	carboxyfluorescein succinimidyl ester
CIEA	Central Institute for Experimental Animals
cμ	cytoplasmic μ chain
DC	dendritic cell
EGFP	enhanced green fluorescent protein
GAPDH	glyceraldehyde 3-phosphate dehydrogenase
HSA	human serum albumin
i.p.	intra-peritoneal
IRES	internal ribosomal entry site
i.v.	intravenous
KLH	keyhole limpet hemocyanin
KO	knockout
MACS	magnetic cell sorting
NOG	NOD/shi-scid/γc^{null}
PE	phycoerythrin
PI	propidium iodide
RT	reverse transcription
SAC	*Staphylococcus aureus* cowan
SP	single positive
TCR	T-cell receptor
γc	γ chain

References

1 Grabstein, K. H., Waldschmidt, T. J., Finkelman, F. D. *et al.* 1993. Inhibition of murine B and T lymphopoiesis *in vivo* by an anti-interleukin 7 monoclonal antibody. *J. Exp. Med.* 178:257.
2 Dittel, B. N. and LeBien, T. W. 1995. The growth response to IL-7 during normal human B cell ontogeny is restricted to B-lineage cells expressing CD34. *J. Immunol.* 154:58.
3 Leonard, W. J., Shores, E. W. and Love, P. E. 1995. Role of the common cytokine receptor gamma chain in cytokine signaling and lymphoid development. *Immunol. Rev.* 148:97.

4 Schraven, B. and Kalinke, U. 2008. CD28 superagonists: what makes the difference in humans? *Immunity* 28:591.
5 Shultz, L. D., Ishikawa, F. and Greiner, D. L. 2007. Humanized mice in translational biomedical research. *Nat. Rev. Immunol.* 7:118.
6 Manz, M. G. 2007. Human-hemato-lymphoid-system mice: opportunities and challenges. *Immunity* 26:537.
7 Legrand, N., Weijer, K. and Spits, H. 2006. Experimental models to study development and function of the human immune system *in vivo*. *J. Immunol.* 176:2053.
8 Payne, K. J. and Crooks, G. M. 2007. Immune-cell lineage commitment: translation from mice to humans. *Immunity* 26:674.
9 Macchiarini, F., Manz, M. G., Palucka, A. K. and Shultz, L. D. 2005. Humanized mice: are we there yet? *J. Exp. Med.* 202:1307.
10 Manning, D. D., Reed, N. D. and Shaffer, C. F. 1973. Maintenance of skin xenografts of widely divergent phylogenetic origin of congenitally athymic (nude) mice. *J. Exp. Med.* 138:488.
11 McCune, J. M., Namikawa, R., Kaneshima, H., Shultz, L. D., Lieberman, M. and Weissman, I. L. 1988. The SCID-hu mouse: murine model for the analysis of human hematolymphoid differentiation and function. *Science* 241:1632.
12 Shultz, L. D., Schweitzer, P. A., Christianson, S. W. *et al.* 1995. Multiple defects in innate and adaptive immunologic function in NOD/LtSz-scid mice. *J. Immunol.* 154:180.
13 Pflumio, F., Lapidot, T., Murdoch, B., Patterson, B. and Dick, J. E. 1993. Engraftment of human lymphoid cells into newborn SCID mice leads to graft-versus-host disease. *Int. Immunol.* 5:1509.
14 Huppes, W., De Geus, B., Zurcher, C. and Van Bekkum, D. W. 1992. Acute human vs. mouse graft vs. host disease in normal and immunodeficient mice. *Eur. J. Immunol.* 22:197.
15 Larochelle, A., Vormoor, J., Hanenberg, H. *et al.* 1996. Identification of primitive human hematopoietic cells capable of repopulating NOD/SCID mouse bone marrow: implications for gene therapy. *Nat. Med.* 2:1329.
16 Ito, M., Hiramatsu, H., Kobayashi, K. *et al.* 2002. NOD/SCID/gamma(c)(null) mouse: an excellent recipient mouse model for engraftment of human cells. *Blood* 100:3175.
17 DiSanto, J. P., Muller, W., Guy-Grand, D., Fischer, A. and Rajewsky, K. 1995. Lymphoid development in mice with a targeted deletion of the interleukin 2 receptor gamma chain. *Proc. Natl Acad. Sci. USA* 92:377.
18 Cao, X., Shores, E. W., Hu-Li, J. *et al.* 1995. Defective lymphoid development in mice lacking expression of the common cytokine receptor gamma chain. *Immunity* 2:223.
19 Ohbo, K., Suda, T., Hashiyama, M. *et al.* 1996. Modulation of hematopoiesis in mice with a truncated mutant of the interleukin-2 receptor gamma chain. *Blood* 87:956.
20 Shultz, L. D., Lyons, B. L., Burzenski, L. M. *et al.* 2005. Human lymphoid and myeloid cell development in NOD/LtSz-scid IL2R gamma null mice engrafted with mobilized human hemopoietic stem cells. *J. Immunol.* 174:6477.
21 Ishikawa, F., Yasukawa, M., Lyons, B. *et al.* 2005. Development of functional human blood and immune systems in NOD/SCID/IL2 receptor {gamma} chain(null) mice. *Blood* 106:1565.
22 Traggiai, E., Chicha, L., Mazzucchelli, L. *et al.* 2004. Development of a human adaptive immune system in cord blood cell-transplanted mice. *Science* 304:104.
23 Hiramatsu, H., Nishikomori, R., Heike, T. *et al.* 2003. Complete reconstitution of human lymphocytes from cord blood CD34+ cells using the NOD/SCID/gammacnull mice model. *Blood* 102:873.
24 Matsumura, T., Kametani, Y., Ando, K. *et al.* 2003. Functional CD5+ B cells develop predominantly in the spleen of NOD/SCID/gammac(null) (NOG) mice transplanted either with human umbilical cord blood, bone marrow, or mobilized peripheral blood CD34+ cells. *Exp. Hematol.* 31:789.
25 Baenziger, S., Tussiwand, R., Schlaepfer, E. *et al.* 2006. Disseminated and sustained HIV infection in CD34+ cord blood cell-transplanted Rag2-/-gamma c-/- mice. *Proc. Natl Acad. Sci. USA* 103:15951.
26 Cosgrove, D., Gray, D., Dierich, A. *et al.* 1991. Mice lacking MHC class II molecules. *Cell* 66:1051.
27 Suemizu, H., Yagihashi, C., Mizushima, T. *et al.* 2008. Establishing EGFP congenic mice in a NOD/Shi-scid IL2Rg(null) (NOG) genetic background using a marker-assisted selection protocol (MASP). *Exp. Anim.* 57:471.
28 Tsuganezawa, K., Kiyokawa, N., Matsuo, Y. *et al.* 1998. Flow cytometric diagnosis of the cell lineage and developmental stage of acute lymphoblastic leukemia by novel monoclonal antibodies specific to human pre-B-cell receptor. *Blood* 92:4317.
29 Kaneko, S., Onodera, M., Fujiki, Y., Nagasawa, T. and Nakauchi, H. 2001. Simplified retroviral vector gcsap with murine stem cell virus long terminal repeat allows high and continued expression of enhanced green fluorescent protein by human hematopoietic progenitors engrafted in nonobese diabetic/severe combined immunodeficient mice. *Hum. Gene Ther.* 12:35.
30 Morita, S., Kojima, T. and Kitamura, T. 2000. Plat-E: an efficient and stable system for transient packaging of retroviruses. *Gene Ther.* 7:1063.
31 Gebe, J. A., Novak, E. J., Kwok, W. W., Farr, A. G., Nepom, G. T. and Buckner, J. H. 2001. T cell selection and differential activation on structurally related HLA-DR4 ligands. *J. Immunol.* 167:3250.
32 Simmons, A. and Jantz, K. 2006. Use of a lentivirus/VSV pseudotype virus for highly efficient genetic redirection of human peripheral blood lymphocytes. *Nat. Protoc.* 1:2688.
33 Sims, G. P., Ettinger, R., Shirota, Y., Yarboro, C. H., Illei, G. G. and Lipsky, P. E. 2005. Identification and characterization of circulating human transitional B cells. *Blood* 105:4390.
34 Imamura, R., Miyamoto, T., Yoshimoto, G. *et al.* 2005. Mobilization of human lymphoid progenitors after treatment with granulocyte colony-stimulating factor. *J. Immunol.* 175:2647.
35 Hystad, M. E., Myklebust, J. H., Bo, T. H. *et al.* 2007. Characterization of early stages of human B cell development by gene expression profiling. *J. Immunol.* 179:3662.
36 Leonard, W. J. and Spolski, R. 2005. Interleukin-21: a modulator of lymphoid proliferation, apoptosis and differentiation. *Nat. Rev. Immunol.* 5:688.
37 Ozaki, K., Spolski, R., Ettinger, R. *et al.* 2004. Regulation of B cell differentiation and plasma cell generation by IL-21, a novel inducer of Blimp-1 and Bcl-6. *J. Immunol.* 173:5361.
38 Choi, E. Y., Jung, K. C., Park, H. J. *et al.* 2005. Thymocyte-thymocyte interaction for efficient positive selection and maturation of CD4 T cells. *Immunity* 23:387.
39 Yahata, T., Ando, K., Nakamura, Y. *et al.* 2002. Functional human T lymphocyte development from cord blood CD34+ cells in nonobese diabetic/Shi-scid, IL-2 receptor gamma null mice. *J. Immunol.* 169:204.
40 Saito, Y., Kametani, Y., Hozumi, K. *et al.* 2002. The *in vivo* development of human T cells from CD34(+) cells in the murine thymic environment. *Int. Immunol.* 14:1113.
41 McCaughtry, T. M., Baldwin, T. A., Wilken, M. S. and Hogquist, K. A. 2008. Clonal deletion of thymocytes can occur in the cortex with no involvement of the medulla. *J. Exp. Med.* 205:2575.
42 Legrand, N., Cupedo, T., van Lent, A. U. *et al.* 2006. Transient accumulation of human mature thymocytes and regulatory T cells with CD28 superagonist in "human immune system" Rag2(-/-) gammac(-/-) mice. *Blood* 108:238.
43 Fortner, K. A. and Budd, R. C. 2005. The death receptor Fas (CD95/APO-1) mediates the deletion of T lymphocytes undergoing homeostatic proliferation. *J. Immunol.* 175:4374.
44 Melkus, M. W., Estes, J. D., Padgett-Thomas, A. *et al.* 2006. Humanized mice mount specific adaptive and innate immune responses to EBV and TSST-1. *Nat. Med.* 12:1316.
45 Tary-Lehmann, M., Lehmann, P. V., Schols, D., Roncarolo, M. G. and Saxon, A. 1994. Anti-SCID mouse reactivity shapes the human CD4+ T cell repertoire in hu-PBL-SCID chimeras. *J. Exp. Med.* 180:1817.
46 Yajima, M., Imadome, K., Nakagawa, A. *et al.* 2008. A new humanized mouse model of Epstein-Barr virus infection that reproduces persistent infection, lymphoproliferative disorder, and cell-mediated and humoral immune responses. *J. Infect. Dis.* 198:673.
47 Kumar, P., Ban, H. S., Kim, S. S. *et al.* 2008. T cell-specific siRNA delivery suppresses HIV-1 infection in humanized mice. *Cell* 134:577.

Published online 8 October 2008

Nucleic Acids Research, 2009, Vol. 37, Database issue ***D863–D867***
doi:10.1093/nar/gkn682

RAPID: Resource of Asian Primary Immunodeficiency Diseases

Shivakumar Keerthikumar[1,2,3], Rajesh Raju[1,2,3], Kumaran Kandasamy[1,3,4], Atsushi Hijikata[5], Subhashri Ramabadran[1,2], Lavanya Balakrishnan[1,2], Mukhtar Ahmed[1], Sandhya Rani[1], Lakshmi Dhevi N. Selvan[1], Devi S. Somanathan[1], Somak Ray[1], Mitali Bhattacharjee[1], Sashikanth Gollapudi[1], Y. L. Ramachandra[3], Sahely Bhadra[6], Chiranjib Bhattacharyya[6], Kohsuke Imai[7], Shigeaki Nonoyama[7], Hirokazu Kanegane[8], Toshio Miyawaki[8], Akhilesh Pandey[1,4], Osamu Ohara[5,9,*] and Sujatha Mohan[1,2]

[1]Institute of Bioinformatics, International Technology Park, Bangalore 560 066, India, [2]Research Unit for Immunoinformatics, Research Center for Allergy and Immunology, RIKEN Yokohama Institute, Kanagawa 230-0045, Japan, [3]Department of Life Science, Kuvempu University, Jnanasahyadri, Shimoga 577 451, India, [4]McKusick-Nathans Institute of Genetic Medicine and Departments of Biological Chemistry, Pathology and Oncology, Johns Hopkins University School of Medicine, Baltimore, MD 21205, USA, [5]Laboratory for Immunogenomics, Research Center for Allergy and Immunology, RIKEN, Yokohama Institute, Kanagawa 230-0045, Japan, [6]Department of Computer Science and Automation, Indian Institute of Science, Bangalore-12, India, [7]Department of Pediatrics, National Defense Medical College, Saitama 359-8513, Japan, [8]Department of Pediatrics, Graduate School of Medicine and Pharmaceutical Sciences, University of Toyama, Toyama 930-0194 and [9]Department of Human Genome Technology, Kazusa DNA Research Institute, Chiba 292-0818, Japan

Received August 15, 2008; Revised September 21, 2008; Accepted September 23, 2008

ABSTRACT

Availability of a freely accessible, dynamic and integrated database for primary immunodeficiency diseases (PID) is important both for researchers as well as clinicians. To build a PID informational platform and also as a part of action to initiate a network of PID research in Asia, we have constructed a web-based compendium of molecular alterations in PID, named Resource of Asian Primary Immunodeficiency Diseases (RAPID), which is available as a worldwide web resource at http://rapid.rcai.riken.jp/. It hosts information on sequence variations and expression at the mRNA and protein levels of all genes reported to be involved in PID patients. The main objective of this database is to provide detailed information pertaining to genes and proteins involved in primary immunodeficiency diseases along with other relevant information about protein–protein interactions, mouse studies and microarray gene-expression profiles in various organs and cells of the immune system. RAPID also hosts a tool, mutation viewer, to predict deleterious and novel mutations and also to obtain mutation-based 3D structures for PID genes. Thus, information contained in this database should help physicians and other biomedical investigators to further investigate the role of these molecules in PID.

INTRODUCTION

Primary immunodeficiency diseases (PIDs) are a class of disorders resulting from intrinsic defects in genes involved in the development and maintenance of the immune system. More than 150 primary immunodeficiency genes are reported thus far, which are classified into eight different categories by the International Union of Immunological Societies (1). Patients with these intrinsic defects have increased susceptibility to recurrent and persistent infections, and they may also have autoimmune and cancer-related symptoms. Most PIDs are rare and the diagnosed patients for a given condition are often randomly spread out around the world (2). The genetic defects that cause PIDs can affect the expression and function of proteins that are involved in a range of biological process such as

*To whom correspondence should be addressed. Tel: +81 45 503 9695; Fax: +81 45 503 9694; Email: oosamu@rcai.riken.jp
Correspondence may also be addressed to Sujatha Mohan. Tel: +81 45 503 7034; Fax: +81 45 503 9694; Email: sujatha@rcai.riken.jp

© 2008 The Author(s)
This is an Open Access article distributed under the terms of the Creative Commons Attribution Non-Commercial License (http://creativecommons.org/licenses/by-nc/2.0/uk/) which permits unrestricted non-commercial use, distribution, and reproduction in any medium, provided the original work is properly cited.

immune development, effector-cell functions, signaling cascades and maintenance of immune homeostasis (3). Recent advances in both diagnosis and therapeutic modalities have allowed these defects to be identified earlier and to be more precisely defined, and they have also resulted in more promising long-term outcomes (4). Development of a freely accessible, dynamic and integrated database with inclusion of genomics, transcriptomics and proteomics data of all genes that are involved in PID has the potential to further accelerate research into PIDs as well as provide physicians with easy access to pertinent clinical and molecular data that is otherwise spread throughout the literature.

Resource of Asian Primary Immunodeficiency Diseases (RAPID) is a web-based compendium of molecular alterations in PIDs that is freely available to the academic community at http://rapid.rcai.riken.jp. It hosts information on the sequence variations mapped to the mRNA and protein sequences for all the genes reported from PID patients worldwide. Besides molecular alterations, RAPID has the protein–protein interaction network from Human Protein Reference Database (HPRD) (5), a database with protein-centric information for all human proteins, along with a graphical representation of the expression of PID genes from microarray profiling of organs and cells of the immune system from Gene Expression Omnibus (GEO) (6) and Reference Database of Immune Cells (RefDIC) (7). In addition, it incorporates mouse studies from Mouse Genome Informatics (MGI) (8) database for the representation of allele-based phenotypes and anatomical systems affected due to either mouse knockouts, knockins and spontaneous mutations for the available PID genes. With inclusion of this variety of data for the PID disease genes, RAPID can serve as a connecting link between the genotype and the phenotype.

RAPID ARCHITECTURE

RAPID is an object-oriented database. We used Zope (http://www.zope.org) for the development of RAPID. Zope is a leading open source web application server and is built using the programming language Python (http://www.python.org). MySQL is used as a backend data storage system.

RAPID allows users access to gene-specific PID information either by using the query page or by browsing. RAPID can be queried by various search options including gene symbol, protein name, mouse phenotypes, chromosome number and PID category, and accession numbers of entries from several database resources. The query system includes an autocomplete option that facilitates quick access to the list of items in the database. Users can browse this resource by PID genes, mutation features such as mutation types and effects. This is the first of its kind database to have these user-friendly features for search and display options.

Primary information page is the default main page of every PID gene in the RAPID. It summarizes the external links available in the public domain such as Entrez (9,10), HPRD, IDR, RefDIC, NetPath, OMIM (11), HGNC (12), PDB (13), Ensembl (14) and UniProt/Swiss-Prot (15). It also includes the disease phenotype linked to the given gene along with the mode of inheritance, alternative names of the gene function and the associated features (Figure 1A).

ANNOTATION OF MUTATION DATA

The sequence variations in PID genes reported from the patients are manually curated by expert biologists from the published literature and mapped to the NCBI RefSeq (16,17) genomic, cDNA and protein sequences to aid the scientific community as per the recommendations for the description of sequence variants by Human Genome Variation Society (HGVS) whose main objectives remain to ensure documentation, collection and free distribution of all variation information (18,19). The main criterion for inclusion of mutation data in the RAPID from the literature is that the PID causing genes mutation analysis has to be performed in patient samples who have already presented with a set of PID clinical presentations or associated features or from cell lines derived from such patients. Carriers and asymptomatic individuals are not included in our annotations.

MUTATION VIEWER

Each entry on the mutation has a link to the mutation viewer, a web-based graphical user interface (GUI) enabled tool named Mutation@A Glance, which can be accessed at http://rapid.rcai.riken.jp/mutBrowse.cgi (Figure 1B). It allows users to visualize the mutation position both at the level of DNA and protein sequences as well as homology based 3D structures with various types of information such as SNP, protein domains and functional sites (Hijikata, *et al.*, manuscript in preparation).

GENE-EXPRESSION PROFILES

Gene-expression profiles of PID genes in various organs and cells of the immune systems from a number of microarray experiments available in public repositories are represented graphically for the available PID gene in the form of histograms with immune cell types along with the corresponding average gene-expression intensity values. This shows the expression pattern of these genes in immune cells, which is of relevance to immunologists (Figure 2A).

INTERACTION NETWORKS

All the primary immunodeficiency disease genes have been mapped to their direct physical interactors and, in turn, these interactors are represented differently based on whether an interactor is already known to be PID or not, any of these interactors have their site of expression in immune cells, or any lethality and/or immune system/hematopoietic phenotypes affected due to either mouse knockout, or spontaneous mutation in mice. This information is graphically represented in the form of nodes and

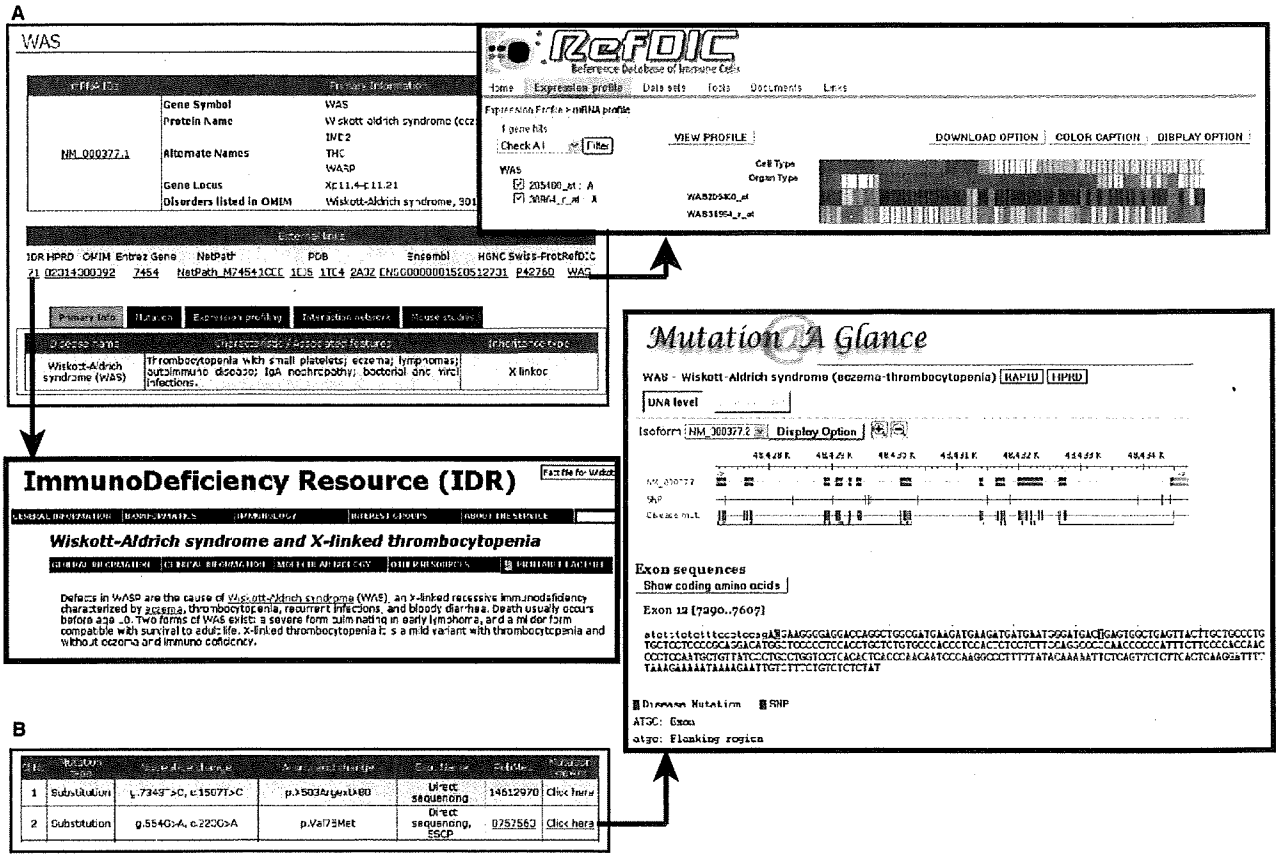

Figure 1. A screenshot of the primary information page and mutation data of *WAS* gene in RAPID. (**A**) Primary information of *WAS* gene along with its external resources to IDR (Immunodeficiency resource) and RefDIC (Reference database of Immune cells) is shown. (**B**) Mutation data curated from the literature reading is shown along with the mutation viewer tool called 'Mutation@A Glance' to visualize the mutations both at DNA and protein levels.

edges with each node having different shapes and colors based on the aforementioned parameters (Figure 2B).

MOUSE STUDIES

The experimental designs to study the effect of the gene variations on the disease phenotype are complicated by the availability of ideal control subjects in case of humans. Mouse models of human diseases are widely used to study genotype–phenotype correlations. In RAPID, all available PID genes are mapped to their corresponding mouse ortholog from MGI to catalog any lethality and/or immune system/hematopoietic phenotypes resulting from knockout of genes or spontaneous mutations (Figure 2C). These features are organized and represented in such a way that RAPID should serve as a discovery tool for prediction of candidate PID genes, a useful feature for immunologists, physicians and researchers.

RAPID STATISTICS

At present, RAPID comprises total of 161 PID genes that are involved in PID, out of which 143 PID genes are reported with over 2455 unique mutation data. Table 1 shows the overall statistics of RAPID as of August 2008.

FUTURE DEVELOPMENTS

In addition to keeping this resource updated on a regular basis and further elucidation of role of PID genes at molecular level, we will initiate global community standard formats for PID data exchange and validation. We will also incorporate standardized DNA diagnosis protocols for screening common PID, which will allow this database to serve as an integrated informational platform for genomics-based PID diagnosis.

CONCLUSIONS

RAPID provides information in an easily accessible and decipherable ways for all users. We support and encourage the input from PID physicians and researcher to share their experiences in standardizing vocabulary terms for representing anonymous patient clinical data that enables RAPID to be used as a diagnostic tool among physicians for early diagnosis and effective treatments

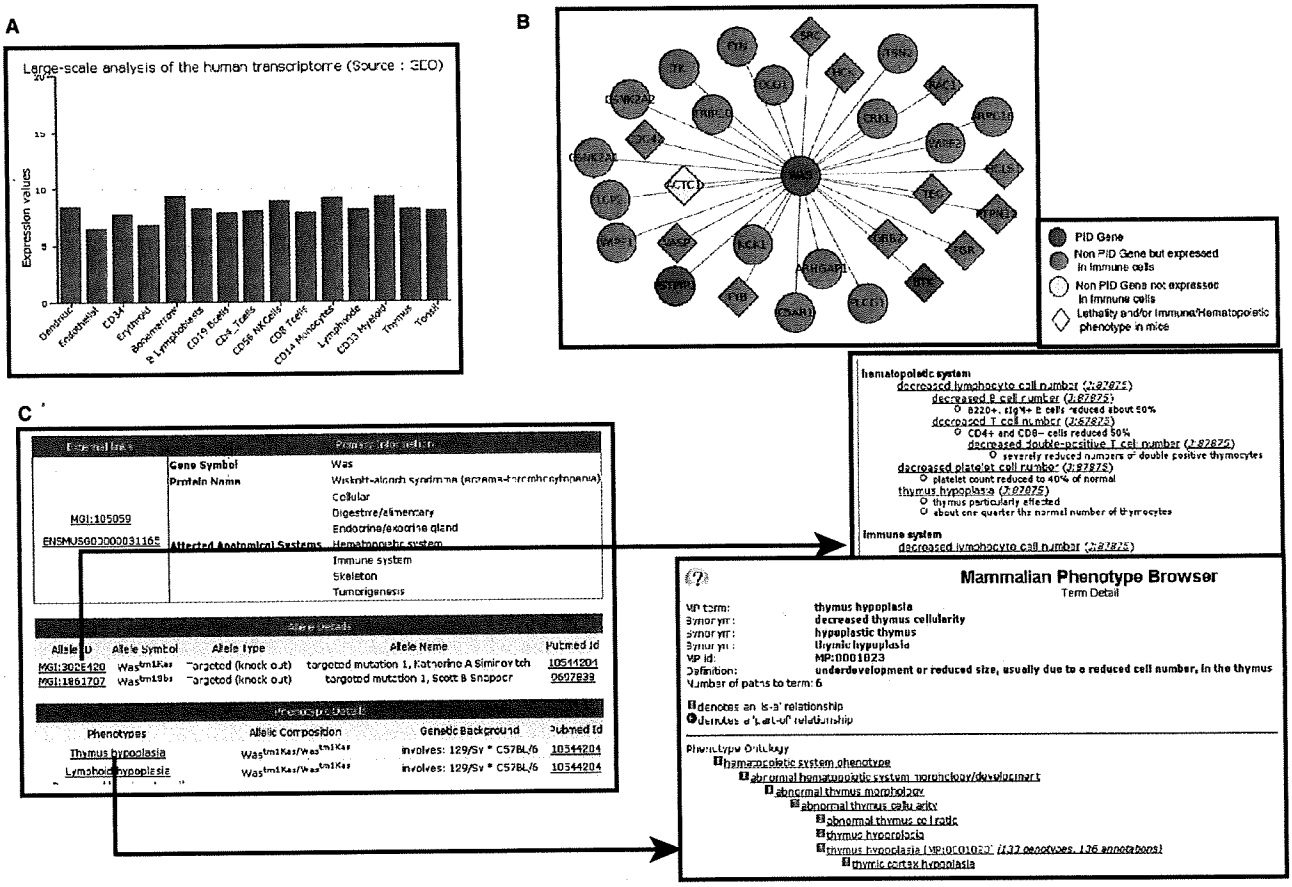

Figure 2. A screenshot of the expression profile, interaction network and mouse studies of *WAS* gene. (**A**) Microarray gene expression profile of *WAS* gene in a particular human microarray data set from GEO. (**B**) Interaction networks of *WAS* from HPRD is shown along with the legends, which explain various parameters of interactors in different shapes and colors. (**C**) Primary information of mouse gene *WAS* is shown along with anatomical systems affected due to mutations and its allelic composition and phenotypes from MGI database.

Table 1. Overall statistics

Number of PID genes	161
Number of PID genes with mutation data	143
Number of non-redundant mutation entries	2455
Number of unique PubMed citations	762

for PID patients. With community participation of interested groups, we anticipate that RAPID will become a primary resource of PIDs in Asia.

ACKNOWLEDGEMENTS

The authors thank Yasuaki Murahashi and Miho Izawa for their help in setting up the web servers, Advanced Center of Computing and Communication (ACCC), RIKEN for providing necessary computing resources, Drs Reiko Kikuno and Fumihiko Ishikawa for their valuable discussion, and all PID physicians involved in the PID Japan project for their valuable input and suggestions.

FUNDING

The Special Coordination Funds for promoting Science and Technology, from the Ministry of Education, Culture, Sports, and Science of Japan. Funding for open access charge: RIKEN Research Center for Allergy and Immunology.

Conflict of interest statement. None declared.

REFERENCES

1. Geha,R.S., Notarangelo,L.D., Casanova,J.L., Chapel,H., Conley,M.E., Fischer,A., Hammarström,L., Nonoyama,S., Ochs,H.D., Puck,J.M. *et al.* (2007) International Union of Immunological Societies Primary Immunodeficiency Diseases Classification Committee. Primary immunodeficiency diseases: an update from the International Union of Immunological Societies Primary Immunodeficiency Diseases Classification Committee. *J. Allergy Clin. Immunol.*, **120**, 776–794.
2. Samarghitean,C., Valiaho,J. and Vihinen,M. (2007) IDR knowledge base for primary immunodeficiencies. *Immunome Res.*, **3**, 6.
3. Marodi,L. and Notarangelo,L.D. (2007) Immunological and genetic bases of new primary immunodeficiencies. *Nat. Rev. Immunol.*, **7**, 851–861.

4. Cunningham-Rundles,C. and Ponda,P.P. (2005) Molecular defects in T- and B-cell primary immunodeficiency diseases. *Nat. Rev. Immunol.*, **5**, 880–892.
5. Mishra,G., Suresh,M., Kumaran,K., Kannabiran,N., Suresh,S., Bala,P., Shivakumar,K., Anuradha,N., Raghunath,R., Madhan Raghavan,T. *et al.* (2006) Human Protein Reference Database - 2006 update. *Nucleic Acids Res.*, **34**, D411–D414.
6. Barrett,T. and Edgar,R. (2006) Gene expression omnibus: microarray data storage, submission, retrieval, and analysis. *Methods Enzymol.*, **411**, 352–369.
7. Hijikata,A., Kitamura,H., Kimura,Y., Yokoyama,R., Aiba,Y., Bao,Y., Fujita,S., Hase,K., Hori,S. *et al.* (2007) Construction of an open-access database that integrates cross-reference information from the transcriptome and proteome of immune cells. *Bioinformatics*, **23**, 2934–2941.
8. Eppig,J.T., Blake,J.A., Bult,C.J., Kadin,J.A., Richardson,J.E. and the members of the Mouse Genome Database Group (2007) The Mouse Genome Database (MGD): new features facilitating a model system. *Nucleic Acids Res.*, **35**, D630–D637.
9. Maglott,D., Ostell,J., Pruitt,K.D. and Tatusova,T. (2005) Entrez Gene: gene-centered information at NCBI. *Nucleic Acids Res.*, **33**, D54–D58.
10. Maglott,D., Ostell,J., Pruitt,K.D. and Tatusova,T. (2007) Entrez Gene: gene-centered information at NCBI. *Nucleic Acids Res.*, **35**, D26–D31.
11. Hamosh,A., Scott,A.F., Amberger,J.S., Bocchini,C.A. and McKusick,V.A. (2005) Online Mendelian inheritance in man (OMIM), a knowledgebase of human genes and genetic disorders. *Nucleic Acids Res.*, **33**, D514–D517.
12. Bruford,E.A., Lush,M.J., Wright,M.W., Sneddon,T.P., Povey,S. and Birney,E. (2008) The HGNC Database in 2008: a resource for the human genome. *Nucleic Acids Res.*, **36**, D445–D448.
13. Dutta,S., Burkhardt,K., Swaminathan,G.J., Kosada,T., Henrick,K., Nakamura,H. and Berman,H.M. (2008) Data deposition and annotation at the worldwide protein data bank. *Methods Mol. Biol.*, **426**, 81–101.
14. Flicek,P., Aken,B.L., Beal,K., Ballester,B., Caccamo,M., Chen,Y., Clarke,L., Coates,G., Cunningham,F., Cutts,T. *et al.* (2008) Ensembl 2008. *Nucleic Acids Res.*, **36**, D707–D714.
15. Boeckmann,B., Bairoch,A., Apweiler,R., Blatter,M.C., Estreicher,A., Gasteiger,E., Martin,M.J., Michoud,K., O'Donovan,C., Phan,I. *et al.* (2003) The SWISS-PROT protein knowledgebase and its supplement TrEMBL in 2003. *Nucleic Acids Res.*, **31**, 365–370.
16. Pruitt,K.D., Tatusova,T. and Maglott,D.R. (2005) NCBI Reference Sequence (RefSeq): a curated non-redundant sequence database of genomes, transcripts and proteins. *Nucleic Acids Res.*, **33**, D501–D504.
17. Pruitt,K.D., Tatusova,T. and Maglott,D.R. (2007) NCBI Reference Sequence (RefSeq): a curated non-redundant sequence database of genomes, transcripts and proteins. *Nucleic Acids Res.*, **35**, D61–D65.
18. Antonarakis,S.E. (1998) Recommendations for a nomenclature system for human gene mutations. Nomenclature Working Group. *Hum. Mutat.*, **11**, 1–3.
19. den Dunnen,J.T. and Antonarakis,S. E. (2000) Mutation nomenclature extensions and suggestions to describe complex mutations: a discussion. *Hum. Mutat.*, **15**, 7–12.

Two Brothers with Ataxia-Telangiectasia-like Disorder with Lung Adenocarcinoma

Naoki Uchisaka, MD, Naomi Takahashi, Masaki Sato, Akira Kikuchi, MD, Shinji Mochizuki, MD, Kohsuke Imai, MD, PhD, Shigeaki Nonoyama, MD, PhD, Osamu Ohara, PhD, Fumiaki Watanabe, PhD, Shuki Mizutani, MD, PhD, Ryoji Hanada, MD, and Tomohiro Morio, MD, PhD

We report on 2 brothers with ataxia-telangiectasia-like disorder with lung adenocarcinoma. They both had ataxia with cerebellar atrophy and mental retardation. They had the same mutation of the *MRE11* gene, which has not been reported previously (c.727T>C and g.24994G>A). *(J Pediatr 2009;155:435-8)*

Ataxia-telangiectasia-like disorder (ATLD) is a rare disease classified under the name of chromosomal breakage syndrome. It is characterized by the clinical features of progressive cerebellar degeneration, increased levels of spontaneously occurring chromosomal aberrations, and increased sensitivity to ionizing radiation with the absence of ocular telangiectasia and immunodeficiency. In 1999, Stewart et al identified *MRE11* mutations from 4 patients with ATLD.[1] Sixteen patients in 6 families have been reported with ATLD.[1-3] Although chromosomal breakage syndromes, such as ataxia-telangiectasia (A-T) and Nijmegen breakage syndrome (NBS), are well known as disorders that predispose patients to malignancy, there has been no earlier report of a patient with ATLD with malignancy. We report on 2 siblings with ATLD in whom lung adenocarcinoma developed.

Case Report

The affected siblings were born to non-consanguineous parents after healthy pregnancies and deliveries. Their parents had a history of diabetes mellitus and smoking, but there was no family history of malignancy.

The brothers had characteristic clinical features of short stature, pointy nose, small jaw, atrophy of the lower legs, and equinus foot deformities. They had cerebellar ataxia, slurred and explosive speech, and ocular apraxia, but did not show any evidence of involuntary movement such as dystonia or dyskinesia. Ataxic gait was noted when they were 2 years old. The boys had been observed for progressive cerebellar ataxia with atrophy of the cerebellum and mental retardation. The degree of cerebellar ataxia and atrophy was more severe in the elder brother, who became wheelchair bound at 6 years of age.

The patients started to speak at 2 years old. One brother's IQ score was 43, and the other's was 75. There was no history of serious infection or evidence of skin or conjunctival telangiectasia. The elder brother was diagnosed with renal Fanconi syndrome; and a renal biopsy showed vacuolar degeneration of the renal tubules.

In 2007, when they were 15 and 9 years old, stage 4 non-small-cell lung cancer (poorly differentiated lung adenocarcinoma with multiple bone metastases) was diagnosed in both boys.

With a laboratory examination, elevation of serum CA125 levels (956.4U/ml and 1449.8U/ml, respectively) and polycythemia were revealed. Serum alpha fetoprotein and immunoglobulin levels were in the reference range (alpha fetoprotein, 5.60 ng/mL and 3.78ng/mLl; immunoglobulin G, 1205 mg/dL and 947 mg/dL). With cytogenetic analysis performed on PHA-stimulated peripheral blood, an increased number of chromosome aberrations, but no specific or particular chromosome abnormalities, was revealed.

Both of the patients received chemotherapy before the diagnosis was made. The elder brother was treated with docetaxel and carboplatin. A half dose of the chemotherapeutic agents was administered because of gastrointenstinal toxicity. He died 11 months after the diagnosis of lung adenocarcinoma.

The younger brother was initially treated with half dose of a docetaxel and cisplatin regimen, and later with irinotecan because of gastrointenstinal toxicity. He also received radiation therapy to the primary tumor. He died 8 months after the diagnosis. Radiation-induced esophagitis was observed in autopsy samples.

ATM deficiency was found to be unlikely, because of the presence of ATM protein that was demonstrated with Western blot analysis (data not shown). We then examined the

A-T	Ataxia-telangiectasia
ATLD	Ataxia-telangiectasia-like disorder
NBS	Nijmegen breakage syndrome

From the Division of Hematology/Oncology, Saitama Children's Medical Center, Saitama, Japan (N.U., A.K., S. Mochizuki, R.H.); Department of Pediatrics, Tokyo Medical and Dental University, Tokyo, Japan (N.T., M.S., F.W., S. Mizutani; T.M.); Department of Pediatrics, National Defense Medical College, Saitama, Japan (K.I., S.N.); and Kazusa DNA Research Institution, Chiba, Japan (O.O.)

This work was supported in part by grants from the Ministry of Health, Labour, and Welfare of Japan (T.M.) and from the Ministry of Education, Culture, Sports, Science Technology of Japan (S. Mizutani and T.M.). The authors declare no conflicts of interest.

0022-3476/$ - see front matter. Copyright © 2009 Mosby Inc. All rights reserved. 10.1016/j.jpeds.2009.02.037

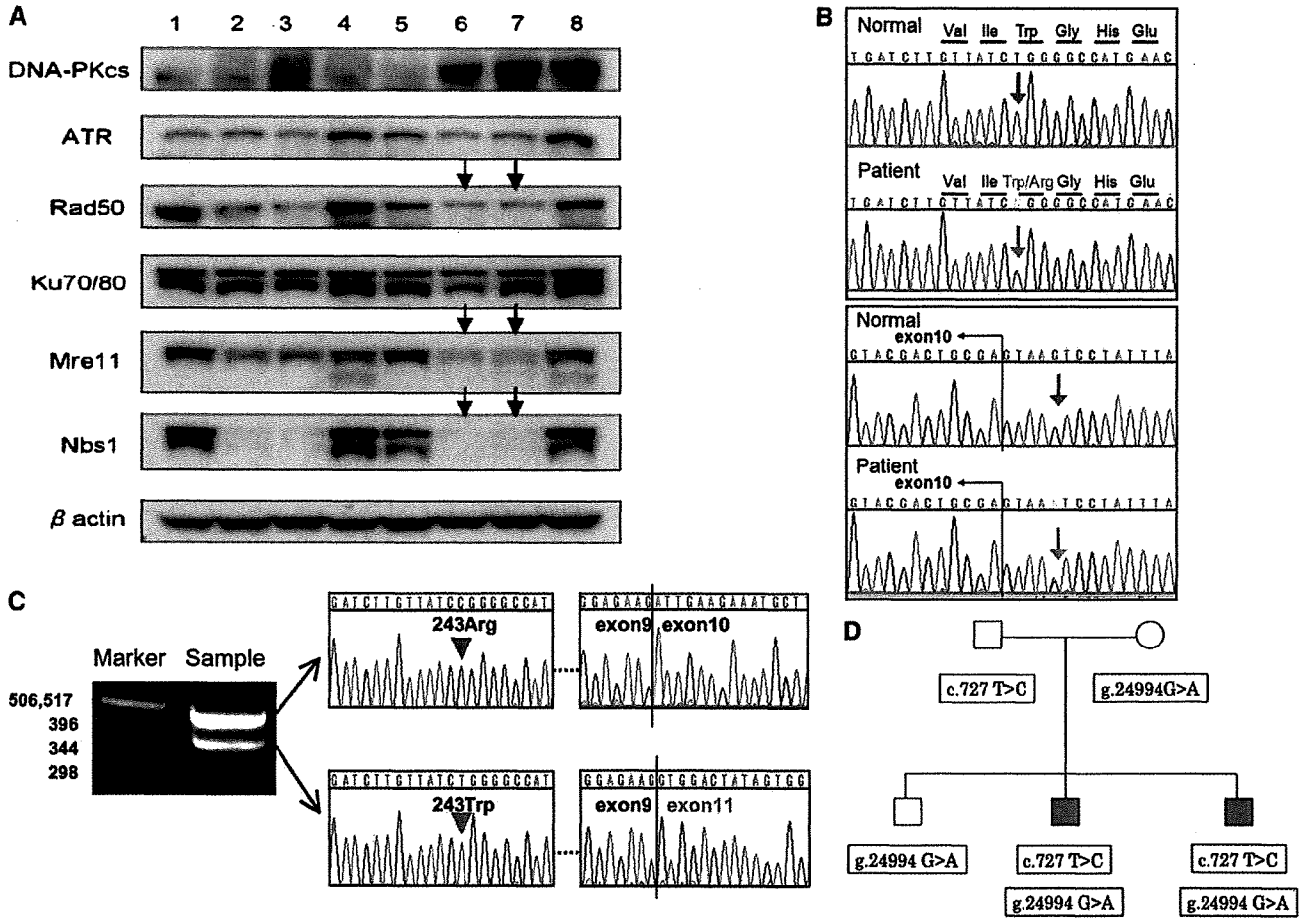

Figure. Mutation analysis of Mre11 deficiency. **A,** Western blot analysis shows alteration in protein levels of Mre11, Nbs1, and Rad50 in the patients. The cell lysates from activated T-cells or EBV-transformed B-cells (EBV-LCL) were subjected to Western blot for detection of indicated proteins. β-actin was included as a control protein to show protein loading in each lane. Lanes 1-4: activated T-cells; Lanes 5-8: EBV-LCL. 1 and 5: healthy control; 2 and 5: elder brother; 3 and 6: younger brother; 4 and 8: A-T patient. **B,** Mutation analysis of *MRE11*. The 20 exons and the flanking intronic regions of *MRE11* gene were sequenced. This revealed c.727 T>C (W243R) in exon 8 and g.24994 G>A in intron 10 that is located 5bp downstream of exon 10, respectively. The sequencing showed T/C in exon 8 and G/A in intron 10; and both mutations are indicated as "N" in the figure. **C,** RT-PCR of exon 7 to exon 11 of *MRE11* cDNA and sequence of the PT-PCR products. Sequencing of 479bp and 398 bp RT-PCR products revealed c. 727 T>C and the deletion of the entire exon 10. **D,** Summary of *MRE11* sequences of the family members.

expression of Mre11, Rad50, and Nbs1 proteins. With the Western blot, severely decreased Nbs1 expression associated with decreased levels of Mre11 and Rad50 was demonstrated in both of the patients (**Figure,** A). Because we failed to detect *NBS1* gene mutation, we looked for alteration in *MRE11* gene in the 20 exons and the flanking intronic sequences. This revealed a T>C substitution in exon 8 and a base substitution of g.24994 G>A in intron 10, 5bp downstream from exon 10 (**Figure,** B). RT-PCR of exon 7–exon 11 of *MRE11* complementary DNA of the patients gave us 2 bands (**Figure,** C). Sequencing of the *MRE11* RT-PCR products revealed a base substitution c.727 T>C in exon 8 in 1 of the alleles and an 81 bp deletion in exon 10 on another allele. The alteration of these DNA sequences predicts an amino acid substitution (W243R) and the loss of 27 amino acids, respectively. The base substitution in intron 10 might have given rise to an alternative splicing of *MRE11*, leading to an in frame 81 bp deletion in exon 10. Thus, the compound heterozygous mutations of *MRE11* gene (c.727 T>C and g.24994 G>A) were identified in both of these brothers (**Figure,** B and C).

The father was a carrier of c.727 T>C mutation, and the mother and their eldest brother were carriers of g.24994 G>A mutation (**Figure,** D). The expression level of Mre11 protein was normal in both of these carriers (data not shown).

Discussion

To date, 16 patients have been reported in 6 families with ATLD (**Table**). Compared with the earlier cases, both of

Table. Clinical features of patients with ataxia-telangiectasia-like disorder

Authors	Year	Nation	Family	Patients	Age at report (years)	Sex	Mutation	Zygosity	Ataxia	Cerebellar atrophy	Ocular apraxia	Telangiectasia	Tumors
Stewart et al	1999	Pakistan	1	1	25	F	633R→Stop	Homozygous	+	+		−	−
				2	20	M			+	+		−	−
		England	2	3	18	M	N117S	Compound heterozygous	+	+	+	−	−
				4	15	M	R571X		+	+	+	−	−
Dalia et al	2004	Italy	3	5	37	M	T481K	Compound heterozygous	+	+	+	−	−
				6	36	F	R571X		+	+	+	−	−
Fernet et al	2005	Saudia Arabia	4	7	37	F	W210C	Homozygous	+	+	+	−	−
				8	33	F			+	+	+	−	−
				9	20	M			+	+	+	−	−
				10	20	M			+	+	+	−	−
			5	11	11	F	W210C	Homozygous	+	+	+	−	−
				12	8	F			+	+	+	−	−
				13	7	F			+	+	+	−	−
			6	14	15	F	W210C	Homozygous	+	+	+	−	−
				15	11	F			+	+	+	−	−
				16	5	F			+	+	−	−	−
This report		Japan	7	17	9	M	W243R	Compound heterozygous	+	+	+	−	+
				18	16	M	Del (I340_R366)		+	+	+	−	+

our patients demonstrated a new clinical feature, lung adenocarcinoma with mental retardation and minor malformations.

The mutations we detected were novel and have not been reported in the earlier cases. The mutation c.727 T>C generates mutant protein with an amino acid substitution of W243R. The mutation g.24994 G>A located 5bp after exon 10 generated a protein that was missing 27 amino acids of exon 10.

These mutations are likely to have crucial influence on the function of MRE11, because they are within the nuclease domain (MRE11 motif IV) and close to the DNA binding domain (407-421), respectively. This *MRE11* gene alteration may be related to the phenotype of our patients: the early onset and rapid progression of the disease, the development of lung adenocarcinoma, and the presence of mental retardation with minor malformations.

In 1995, the *MRE11* gene was isolated by Petrini et al.[4] The gene is consisted of 20 exons and located at 11q21. MRE11 protein interacts with RAD50 and NBS1 proteins and forms a core of MRN complex. The MRN complex is important for double-strand break repair, meiotic recombination, and telomere maintenance.[5] The complex acts not only as a transducer of the signal from activated ATM protein, but also as a stimulator of ATM protein in the early phase of the double-strand break response.[6] These studies explain the clinical and biological resemblance among A-T, NBS, and ATLD.

A-T is well known as a disorder with predisposition to malignancy such as lymphoid tumor and several types of adenocarcinoma.[7,8] The lifetime prevalence of cancer in patients with A-T is 10% to 30%. NBS is also known as a disorder with predisposition to malignancy of the lymphoid organ.[9] In these disorders, increased frequency of tumors can be explained by increased genome instability. The genomic instability arises from defective recognition and repair of double-strand DNA breaks and from defective cell cycle checkpoints. Although these disorders share common clinical features as a genomic instability syndrome, there has been no report of malignancy in patients with ATLD. Association of *MRE11* mutations/polymorphisms with lung adenocarcinoma has not been reported, and insufficient data is available to assess the role of genetic change of *MRE11* in cancer and cancer risk at this point.

Although further detailed biochemical study is required for delving into the pathogenesis of lung carcinoma in our patients with MRE11 deficiency, this report suggests a possible risk of malignancy associated with *MRE11* genotype in patients with ATLD. ■

Submitted for publication Oct 24, 2008; last revision received Jan 15, 2009; accepted Feb 17, 2009.

Reprint requests: Tomohiro Morio, MD, PhD, 1-5-45 Yushima, Bunkyo-ku, Tokyo 113-8519, Japan. E-mail: tmorio.ped@tmd.ac.jp.

References

1. Stewart GS, Maser RS, Stankovic T, Bressan DA, Kaplan MI, Jaspers NG, et al. The DNA double-strand break repair gene hMRE11 is mutated in individuals with an ataxia-telangiectasia-like disorder. Cell 1999;99: 577-87.
2. Delia D, Piane M, Buscemi G, Savio C, Palmeri S, Lulli P, et al. MRE11 mutations and impaired ATM-dependent responses in an Italian family with ataxia-telangiectasia-like disorder. Hum Mol Genet 2004;13: 2155-63.
3. Fernet M, Gribaa M, Salih MA, Seidahmed MZ, Hall J, Koenig M. Identification and functional consequences of a novel MRE11 mutation

affecting 10 Saudi Arabian patients with the ataxia telangiectasia-like disorder. Hum Mol Genet 2005;14:307-18.
4. Petrini JH, Walsh ME, DiMare C, Chen XN, Korenberg JR, Weaver DT. Isolation and characterization of the human MRE11 homologue. Genomics 1995;29:80-6.
5. Carney JP, Maser RS, Olivares H, Davis EM, Le Beau M, Yates JR III, et al. The hMre11/hRad50 protein complex and Nijmegen breakage syndrome: linkage of double-strand break repair to the cellular DNA damage response. Cell 1998;93:477-86.
6. Uziel T, Lerenthal Y, Moyal L, Andegeko Y, Mittelman L, Shiloh Y. Requirement of the MRN complex for ATM activation by DNA damage. EMBO J 2003;22:5612-21.
7. Hecht F, Hecht BK. Cancer in ataxia-telangiectasia patients. Cancer Genet Cytogenet 1990;46:9-19.
8. Taylor AM, Metcalfe JA, Thick J, Mak YF. Leukemia and lymphoma in ataxia telangiectasia. Blood 1996;87:423-38.
9. The International Nijmegen Breakage Syndrome Study Group. Nijmegen breakage syndrome. Arch Dis Child 2000;82:400-6.